



# A quantitative assessment of the behavior of metallic elements in urban soils exposed to industrial dusts near Dunkerque (northern France)

Marine Casetta<sup>1</sup>, Sylvie Philippe<sup>1</sup>, Lucie Courcot<sup>1</sup>, David Dumoulin<sup>2</sup>, Gabriel Billon<sup>2</sup>, François Baudin<sup>3</sup>,  
Françoise Henry<sup>1</sup>, Michaël Hermoso<sup>1</sup>, and Jacinthe Caillaud<sup>1</sup>

<sup>1</sup>LOG, Laboratoire d'Océanologie et de Géosciences, Université du Littoral Côte d'Opale, Université de Lille,  
CNRS, IRD, UMR 8187, 62930 Wimereux, France

<sup>2</sup>Univ. Lille, CNRS, UMR 8516 – LASIRE, Laboratoire Avancé de Spectroscopie pour les Interactions,  
la Réactivité et l'Environnement, 59000 Lille, France

<sup>3</sup>Sorbonne Université – CNRS, UMR 7193 IStEP – Institut des Sciences de la Terre de Paris,  
75005 Paris, France

**Correspondence:** Marine Casetta (marine.casetta@univ-littoral.fr)

Received: 20 June 2024 – Discussion started: 14 October 2024

Revised: 3 March 2025 – Accepted: 28 March 2025 – Published: 4 July 2025

**Abstract.** In urban and industrialized areas, soil contamination and degradation caused by industrial dust deposition may pose significant health and environmental risks. Generally, the mobility and thus bioavailability of potentially toxic elements (PTEs) are key factors in these issues. In the Dunkerque agglomeration, one of the most industrialized regions in France, the soils are periodically exposed to metallurgical dust fallout, rich in PTEs. However, no study has reported on the behavior of these PTEs once integrated into the soils. The aim of this study is therefore to assess the fate of PTEs in the urban soils of Dunkerque in terms of vertical migration and potential bioavailability.

Four soil short cores were collected in the city of Gravelines (Dunkerque agglomeration) along a gradient from industrial emitters to deposition sites. Each soil core was cut into discrete 1 cm sections for PTE concentration analyses (ICP-AES/MS). Single HCl extractions were performed to evaluate PTE mobility in soils and their behavior according to the current soil parameters. For this purpose, key soil properties were identified, including grain-size distribution, mineralogy, pH, cation exchange capacity (CEC), TOC (total organic carbon), calcium carbonates and water contents in addition to the soil chemical composition (XRF, ICP-AES/MS).

The studied soils revealed globally low absorbent capacities for pollutants (CEC averaging 5.3 meq/100 g), partially counterbalanced by the buffering effect of calcium carbonates (contents ranging from 8 %–30 %). Near the industrial emitters, minor ( $1 < EF < 3$ ) to moderately severe ( $5 < EF < 10$ ) enrichment factors (EFs) were highlighted for industrial PTE (Cr, Ni, Mo, Mn, Cd and Zn) in the top 3 cm of soils near the industrial emitters. The contamination profiles of these soils are assigned to atmospheric inputs of metallurgical dust. Using a relatively strong leaching reagent (1 M HCl), we estimated a low vertical mobility for Cr, Ni and Mo (average leached ratios  $< 25\%$ ) in soils, suggesting their association with refractory phases (natural or anthropogenic). In contrast, Mn, Cd and Zn, which are related to industrial and/or urban sources, present a higher mobility (average leached ratios  $> 60\%$  for Mn and Cd and about 44 % for Zn).

Our study points out the stability of industrial PTEs in soils under the current physicochemical conditions (calcareous soils with a slightly basic pH of 7.8). In this context, the monitoring of industrial PTEs in these urban soils is highly recommended, considering (1) the presence of allotment gardens in the vicinity of emitters and (2) the potential evolution of soil conditions due to increasing flood events.

## 1 Introduction

Soils are essential to the survival of civilizations and terrestrial ecosystems although they are extremely vulnerable and nonrenewable at the scale of human life (Minami, 2009; Smith et al., 2015; Stavi et al., 2016). The Food and Agriculture Organization of the United Nations recently recorded 5 670 million ha of land worldwide in declining biophysical conditions (FAO and UNEP, 2021). This report indicates that human activities are responsible for more than 29 % of this deterioration through changes in land uses, soil over-exploitation, climate change, introduction of invasive exotic species or release of pollutants (Emadodin and Bork, 2012; Tetteh, 2015; Dror et al., 2022).

Among the various soil pollutants, potentially toxic elements (PTEs) are particularly studied because of the threat that they represent to the ecosystems and human health. This is especially the case when they are mobilized and transferred to groundwater or the food chain (Zhuang et al., 2009; Rajmohan et al., 2014; Sun et al., 2018). Soils act as key interfaces between several environmental compartments, and their physicochemical properties make them both vectors and reservoirs for contaminants (Girard, 2005; Kandpal et al., 2005; Palansooriya et al., 2020; Sarkar et al., 2021). In urban areas, anthropogenic activities significantly contribute to soil pollution by PTEs, especially in metallurgical activities and mostly via atmospheric deposits (Duzgoren-Aydin et al., 2006; Khademi et al., 2019; Manta et al., 2002). The resulting soil degradation by PTE inputs may cause major health and environmental problems, particularly in areas of increasing density of population (Schulin et al., 2007; Douay et al., 2013; Ortega Montoya et al., 2021).

In the Dunkerque agglomeration (northern France), over 150 plant facilities constitute a major risk for the environment. In 2021, the local metallurgical industries emitted more than 2700 t of total dust into the atmosphere, pinpointing concerns about the contamination of the surrounding soils (Géorisques, 2023b). To date, only one study has focused on the soils of this area, investigating the spatial distribution of PTEs in surficial soils in the city of Gravelines (Dunkerque agglomeration) (Casetta et al., 2024). This study provided critical insights, highlighting (1) an appreciable portion of coals, iron ores, slags and other metallurgical products (> 88 %) in the industrial dust falling in the streets of the city during northeast wind and dry periods; (2) a diffuse contamination of soils by PTEs associated with industrial dust, such as Cr, Ni and Mo in particular but also Zn, Cd and Mn; and (3) the punctual degradation of the soil quality by industrial dust.

While this previous work revealed the contamination of surface soils by industrial dust, two main questions remain. They relate to the vertical distribution of the metallic contaminants in the soil profiles and to the capacity of these soils

to retain pollutants. These points are crucial, as understanding the behavior of industrial PTEs is essential to evaluate their long-term environmental impact, including their potential transfer to groundwater and uptake by biota. The present study is the first to investigate the vertical distribution and possible leaching of PTEs (Cr, Mn, Ni, Cu, Zn, Mo and Cd) associated with industrial dust or anthropogenic inputs in selected urban soils (Gravelines). To evaluate the mobility of PTEs, single HCl extractions were carried out on four soil short cores (0–11 cm). In addition, their physicochemical profiles were established, including grain-size distribution, water content, pH, cation exchange capacity (CEC), calcium carbonates, total organic carbon (TOC), major oxide concentrations and mineralogical composition. Using these parameters has the purpose of better understanding the interactions between PTEs and the soil matrix. Finally, this work seeks to highlight the specific behavior of PTEs in soils and their potential link with industrial sources.

## 2 Material and methods

### 2.1 Study area and sampling

The city of Gravelines (50°59' N, 2°08' E) is located in northern France on the North Sea coast (Fig. 1); it has a surface area of 22.66 km<sup>2</sup>, and its population was 11 014 in 2019 (INSEE). The climate is temperate: average annual rainfall of 727 mm and annual temperature ranging between 2 and 22 °C (MERRA-2 meteorological data, 1980–2016). The land use distribution is 52 % of urbanized/industrialized spaces, 22 % of agricultural, 16 % of natural spaces and 10 % of infrastructures. Three metallurgical production sites and one plant for receiving, handling and storing ores in the open air were installed less than 5 km from the city center as result of the construction of the seaport of Dunkerque (industrialized seaport in Fig. 1). The soils of the studied zone were developed on Holocene marine and alluvial clay and sandy sediments deposited during the Gallo-Roman medieval period and belonging to the Flanders coastal plain (Leplat et al., 1988). In this plain, the soils mainly consist of clayey–sandy materials and are rich in calcium carbonates (median value: 13 %) (Sterckeman et al., 2004). According to the pedological classification of the French Association for Soils Study (AFES), the soils of Gravelines can be ascribed to Thalassosols, which are characteristic of a pedogenetic evolution on marine or alluvial deposits (Baize and Girard, 2009; GIS Sol and RMT Sols et Territoires, 2019). In the World Reference Base for Soil Resources (WRB) system (FAO, 2014), they can be classified as Solonchaks, reflecting their development in coastal environments. In this highly populated studied area, the coastal plain is drained through a dense network of channels to avoid flooding from the sea or by brackish water/freshwater. Thus, the characteristics of the studied soils

may locally significantly differ from the general type proposed (i.e., Solonchaks).

Four sampling stations were selected in the city of Gravelines (Fig. 1) according to (1) the concentrations of PTEs associated with industrial dust fallout (Casetta et al., 2024), (2) the nature of the soil matrices, and (3) their distance to the emission sources. They present two types of uses: collective use as parks and green spaces in the city center (station 1) and mesophilic grassland or deciduous planting trees located near the industrial emitters (stations 2, 3 and 4). Short cores of soils under herbaceous cover were collected at the four stations in July 2021 during the summer season using a manual auger and PVC tubes. For each site, one core (diameter of 4.5 cm and depth of 11 cm in order to sample the upper A horizon) was taken and cut into 1 cm sections using a Teflon core cutting table. Thus, a total of 44 soil samples were analyzed.

## 2.2 Nature of the soil matrices

### 2.2.1 General soil parameters

The water content of the soils was determined by weighing samples before and after drying a 30 g aliquot at 65 °C in a ventilated oven (according to the normative protocol NF EN 1097-5). A combined glass electrode and a pH meter were used to measure soil pH in deionized water (1 : 5 soil : solution) (NF ISO 10390; see Goix et al., 2015). The soil cation exchange capacity (CEC) was determined using a spectrophotometric method based on cobaltihexamine chloride absorbance (Aran et al., 2008). Aliquots of 2 g of dry samples were mixed into a 0.01 N solution of cobaltihexamine chloride over 1 h. The solution was filtered through 0.22 µm filters (cellulose acetate) after 10 min centrifugation (4000 g). The CEC was obtained by measuring the absorbance at 472 nm of the collected mixture.

The grain-size distribution and calcium carbonate content were measured in the subsurface (0–1 cm), the middle (4–5 cm) and a deeper layer (9–10 cm) for the four sampled cores. The grain-size distribution was determined on wet samples by laser diffraction. The Coulter LS 13 320 instrument (gallium arsenide, 750 nm wavelength, Brea, USA) measured a particle diameter ranging from 0.375–2000 µm. Prior to analysis, organic matter was removed by adding 50 mL of H<sub>2</sub>O<sub>2</sub> (35 %) according to the Belgian standard NBN 589-207 Sect. 3 (Leifeld and Kögel-Knabner, 2001; Amar et al., 2021). A 2 mm mesh sieve was used to remove the higher size fraction and each soil sample was sonicated to achieved disaggregation. Particle size classes were assigned according to the Soil Science Division Staff (2017) grain-size scale, i.e., 0.375–2.0 µm for the clay fraction, 2.0–20 µm for the fine silt fraction, 20–50 µm for the coarse silt fraction and 50–2000 µm for the sand fraction. A manual calcimeter (OFITTE, Houston, USA; dried and ground samples) was calibrated with pure calcium carbonate to obtain the total

carbonate content (CaCO<sub>3</sub>) of the soil samples. This content was estimated by the gas pressure emitted after a reaction of 1 g of fine powdered sample when adding 20 mL of HCl 20 %. Measurement uncertainties were estimated from three analytical replicates performed using the highest and lowest values during laboratory phases. The absolute uncertainties for the studied soil parameters are as follows: pH ± 0.1, CEC ± 0.2 meq/100 g, CaCO<sub>3</sub> content ± 1 %, particle size distribution: clay ± 0.5 %, fine silt ± 2 %, coarse silt ± 2 % and sand ± 3 %.

### 2.2.2 Total organic carbon (TOC) content and characterization by Rock-Eval measurements

The soil samples were analyzed with a Rock-Eval 6 (RE6) Turbo device (Vinci Technologies, Nanterre, France) using the basic setup for soil organic matter analysis (Disnar et al., 2003; Hetényi and Nyilas, 2014). The RE6 technique required two steps: (1) the pyrolysis of 60 mg of finely ground soil (< 250 µm) in an N<sub>2</sub> atmosphere (from 200–650 °C; heating rate of 30 °C min<sup>-1</sup>) followed by (2) the oxidation of the pyrolysis residues in an oxygenated atmosphere (from 300–850 °C; heating rate of 20 °C min<sup>-1</sup>). Volatile hydrocarbon (HC) effluents during pyrolysis were detected and quantified using flame ionization detection (FID), while oxygen compounds (CO, CO<sub>2</sub>) were quantified during the two steps by infrared detection. Measurements resulted in the production of five thermograms (S1 to S5) per sample, corresponding to free hydrocarbons (S1), pyrolyzable hydrocarbons (S2), CO<sub>2</sub> and CO (S3) generated during the pyrolysis step and to CO and CO<sub>2</sub> (S4 for organic residual carbon and S5 for mineral carbon) produced during the oxidation step. The complete description of the method is available in Lafargue et al. (1998) and Cécillon et al. (2018). Finally, the analysis of the different thermograms allowed for the calculation of several parameters (Espitalié et al., 1977, 1985; Vandembroucke and Largeau, 2007) as

- the total organic carbon content (TOC; wt %) corresponding to the sum of residual and pyrolyzed organic carbon;
- the hydrogen index (HI; mg HC/g TOC) corresponding to the quantity of HC released relative to TOC (S2/TOC);
- the oxygen index (OI<sub>RE6</sub>; mg O<sub>2</sub>/g TOC) corresponding to the quantity of oxygen released as CO and CO<sub>2</sub> during pyrolysis and relative to TOC and calculated as follows (Lafargue et al., 1998):

$$OI_{RE6} = \left[ \left( \frac{16}{28} \times OI_{CO} \right) + \left( \frac{32}{44} \right) \times OI_{CO_2} \right],$$

with  $OI_{CO} = 100 \times S3_{CO}/TOC$  and  $OI_{CO_2} = 100 \times S3_{CO_2}/TOC$ .

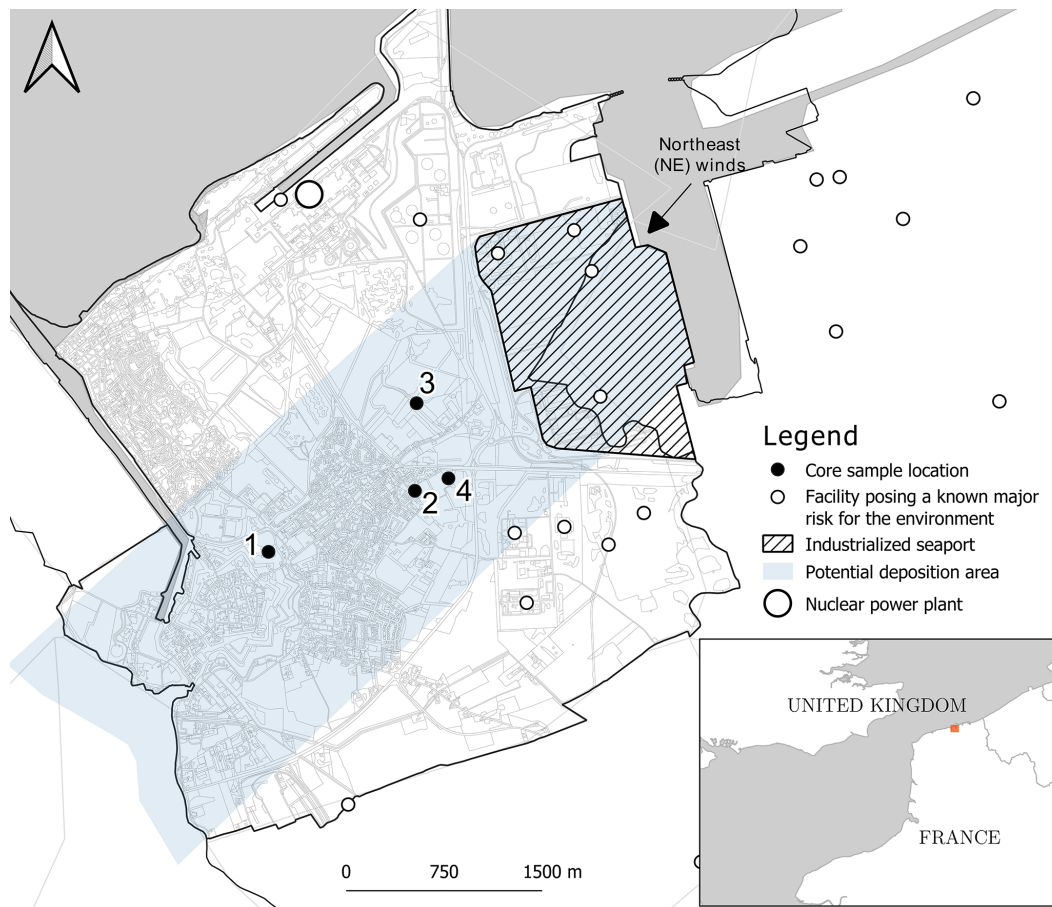


**Figure 1.** Map of the city of Gravelines indicating the sampling stations located southwest of the industrialized seaport (IGN – BD TOPO® Nord 2023).

HI and  $OI_{RE6}$  are used to highlight the main type of organic matter present in the studied soils. For this purpose, these indices are compared to the van Krevelen diagram (H / C vs. O / C) of Espitalié et al. (1977).

### 2.2.3 Major oxide measurement

An energy dispersive X-ray fluorescence spectrometer (Bruker S2 PUMA ED-XRF) was used to measure the concentration of seven major oxides ( $Na_2O$ ,  $MgO$ ,  $Al_2O_3$ ,  $SiO_2$ ,  $K_2O$ ,  $CaO$  and  $Fe_2O_3$ ) in fused soil beads. The spectrometer was equipped with a 50 kV Ag anode tube (maximum power: 50 W, maximum high voltage: 50 kV, maximum current: 2 mA, cooling medium: air) and a high-resolution silicon drift detector ( $< 141$  eV for  $Mn K\alpha_1$ ). Spectral data were analyzed by Spectra Elements software version 2.0. Soil samples were dried, sieved (2 mm), ground, homogenized and calcined at  $1050^\circ C$  (loss on ignition, LOI). Then, fused bead specimens were formed by mixing 500–1000 mg of calcinated powder with a lithium tetraborate (33 %), lithium metaborate (67 %) and lithium bromide ( $< 1\%$ ) mixture. These flux mixtures were loaded in a Katanax® K1 Prime

fluxer and heated up to  $1060^\circ C$  for 20 min. Analytical quality of the XRF measurements was controlled by analyzing 11 certified samples of stream sediments. Determination limits (DLs) and measurement uncertainties are available in Table S1 in the Supplement.

### 2.2.4 Mineralogy

Mineralogy X-ray diffraction (XRD) studies were carried out using an AXS D4 endeavor diffraction system (Bruker; 35 kV, 30 mA;  $Cu K\alpha$  radiations) coupled to a PSD Lynx-Eye detector. Crushed soil samples were examined as random total powder to obtain the total mineralogical composition between  $3$  and  $60^\circ 2\theta$ . Background stripping, diffraction peak indexing, mineral identification by comparison with the files of the Joint Committee on Powder Diffraction Standards (JCPDS) and semi-quantitative analysis were carried out using the X'Pert data HighScore software. Thus, a list of four minerals (Table S2 in the Supplement) was chosen according to (1) the best match between the positions of peaks (score) and (2) the quality of the reference based on a calibration with titanium (reference intensity ratio, RIR). For the

clay preparation, 0.2 M hydrochloric acid was used to decalcify the soil samples, and the excess acid was removed by repeated centrifugations after rinsing with deionized water. Settling was used to isolate the clay-sized fraction ( $< 2 \mu\text{m}$ ), which was next oriented on glass slides (oriented mounts). Clay minerals are identified between  $2.5$  and  $32^\circ 2\theta$  according to the position of the (001) series of basal reflections on air-dried, glycolated (after saturation for 12 h in ethylene glycol) and  $490^\circ\text{C}$  heated (for 2 h) diffractograms (Holtzapffel, 1985). Their semi-quantification was carried out on the glycerol curve using MacDiff software. The reproducibility of technical works and measurements was tested, and the relative error was  $< 5\%$  (Bout-Roumazeilles et al., 1999).

### 2.3 Vertical evolution of PTE concentrations

#### 2.3.1 PTE concentrations in total and leached soil samples

An amount of 200 mg of each ground soil samples were digested using first a concentrated HF–HNO<sub>3</sub> mixture (67 : 33 ratio of  $v : v$ ) and then two successive concentrated HCl–HNO<sub>3</sub> mixtures (67 : 33 ratio of  $v : v$ ). Each digestion step lasted 48 h at  $125^\circ\text{C}$  before evaporation. Dissolved samples were finally diluted in 9 mL with acidified ultrapure MilliQ® (Millipore 18.2 MΩ cm resistivity) water. Each solution was filtered using 0.22 μm filters (cellulose acetate) to remove potential residues. All the reagents were of the optimal/Suprapur grade. Single extractions were performed on the same ground soil samples by mixing 1 g of powder with 20 mL of cold 1 M HCl for 24 h (Billon, 2001; Philippe et al., 2008). Next, leached samples were centrifuged, and the supernatant was filtered on 0.22 μm filters (cellulose acetate) for ICP analyses. This leaching approach using 1 M HCl was chosen to match with the high calcium carbonate content of the studied soils (12 %–30 %), relatively young and developed on Holocene coastal sediments (deposited during the Gallo-Roman medieval period). Indeed, weaker acid concentrations (0.2–0.5 M) and shorter contact time (Madrid et al., 2007; Kubová et al., 2008; Pelfrène et al., 2020) could underestimate PTE mobility in the leaching solution due to buffering effects of carbonates (Birch, 2017). The 1 M HCl extractions is thus supposed to leach, from the soils, metals potentially mobilized through local changes in pH: exchangeable metals, metals weakly bound to organic substances (Waterlot et al., 2017; Pelfrène et al., 2020), metals precipitated with calcium carbonates or associated with amorphous, or poorly crystallized Fe–Mn oxides or hydroxides (Yong et al., 1992; Rao et al., 2010). According to Hamdoun et al. (2015) and Yu et al. (2021), this technique allows for the estimation of the general mobility and reactivity of PTEs in the soil matrices. The total content of the studied PTEs was determined in both total and leaching solutions using ICP-AES (Agilent 5110 VDV for Cu) and ICP-MS (Agilent 7850 for Cr, Mn, Ni, Zn, Mo and Cd). The accuracy and precision were controlled

using 2 sediment standard reference materials (MESS-3 and PACS-2), 12 analytical triplicates and 6 blank samples. The recovery values of the reference standards and the detection limits are available in Table S3 in the Supplement. To discuss the PTE mobility in soils, Table 1 summarizes their environmental characteristics (uses, environmental sources and pathways, mobility in relation to environmental conditions). Considering these data, what is expected in the studied soils is a high mobility for Cu, Mn, Mo, Ni, Zn and to a lesser extent Cd and a low mobility for Cr after 1 M HCl leaching.

#### 2.3.2 PTE enrichment factors (EFs)

Trace metal concentrations were compared to those of agricultural plowed soils of the French Flemish Coastal Plain (the so-called Wateringues marine plain), which is supposed to be preserved from potential contamination sources (because it is distant from industrial activities, busy roads and houses) (Sterckeman et al., 2004). EFs evaluate the degree of metallic contamination of soils by distinguishing anthropogenic from natural metal concentrations (Ye et al., 2011; Harb et al., 2015). Aluminum (Al) is commonly used as a normalizing element (Brady, 1984; Duodu et al., 2017). In this sense, EFs were calculated following Eq. (1):

$$EF = \frac{C_n/C_{Al}}{B_n/B_{Al}}, \quad (1)$$

where  $C_n$  and  $C_{Al}$  are the concentration of a metal element  $n$  and the concentration of Al in the sample, respectively, and  $B_n$  and  $B_{Al}$  are the concentration of a metal element  $n$  and the concentration of Al in the Wateringues marine plain background (median values of the agricultural soils from Sterckeman et al., 2004), respectively.

### 2.4 Data analysis

Maps were made using QGIS 3.10 (QGIS Development Team, 2023). Statistical computing and graphics were performed on R software (R Core Team, 2022) using the following packages: FactoMineR (Lê et al., 2008), ggplot2 (Wickham, 2016), corTest (Yu et al., 2020), factoextra (Kassambara and Mundt, 2020) and corrplot (Wei and Simko, 2021). As suggested by Chapman (1996), all concentration values below the detection limit (DL) were replaced by half of the DL for the statistical analyses. As the collected data present a non-parametric distribution, the correlations between results were highlighted using the Spearman's correlation test ( $R$ ).

## 3 Results

### 3.1 Soil cores properties

#### 3.1.1 Physicochemical parameters

The physicochemical properties of the soil cores are available in Table 2. The study of soil parameters reveals signifi-

**Table 1.** Environmental geochemistry of the studied PTEs (after Goldberg et al., 1996; Baize, 1997; Reimann and De Caritat, 1998; Crea et al., 2013).

Element	Environmental sources and pathways	Mobility in soils			
		Acidic conditions	Alkaline conditions	Oxidizing conditions	Reducing conditions
Cr	Steel works (stainless steel, alloys, chrome plating), electrometallurgy, combustion of natural gas, oil and coal, agriculture (some P fertilizers)	very low	very low	very low	very low
Mn	Steel production, mining and smelting, traffic (antiknock agent in gasoline), agriculture (fertilizers, fungicides), rock weathering, windblown dust	high	very low	very low	high
Ni	Steel works (alloys, electroplating), petroleum refining, catalysis, traffic, fuel/coal combustion, agriculture (fertilizers)	high	very low	medium	medium
Cu	Cu mining and smelting, other non-ferrous smelters, electrical industry, plastic industry, steel works (alloys), sewage sludge, agriculture (pesticides, manure), geogenic dust, rock weathering	very high	very low	medium	very low
Zn	Zn smelters, galvanizing, alloys, combustion, traffic, wastewater, roof, agriculture (pesticides, manure), geogenic dust	high	very low	high	very low
Mo	U mining, Mo mining and smelting, alloys, oil refining, oil and coal combustion, sewage sludge, phosphate detergents, agriculture (P fertilizers), geogenic dust, weathering	high	very high	high	very low
Cd	Coal combustion, iron and steel mills, electroplating, Pb smelting, incinerators, traffic, sewage sludge, agriculture (fertilizers)	relatively high	medium	variable	very low

cant variations between the four sampled stations and along depth profiles. Soil pH from all sampled stations is slightly basic (range: 7.4–8.3, average value: 7.8). Notable heterogeneity in soil textures is highlighted between cores. Core 1 presents a “sandy loam” texture with the highest sand contents (40%–58%) and the lowest clay contents (9%–12%). Conversely, cores 3 and 4 are characterized by a “silt loam” texture, higher clay contents (13%–19%) and lower sand values (8%–26%). Core 2 presents an intermediate “loam” texture with clay and sand values ranging from 12%–16% and from 31%–41%, respectively (Richer-De-Forges et al., 2008). No important vertical variation is observed in the grain-size distribution of soil cores, except in core 4, in which clay content increases in the subsurface in an inverse proportion to sand content.

The CEC values range from 3.5–7.3 meq/100 g and are globally low, according to Rengasamy and Churchman (1999). Maximal CEC values are measured in the subsurface of cores 3 and 4 (0–1 cm; 7.3 and 6.8 meq/100 g, respectively), while minimum CEC is measured in core 2 (10–11 cm) (3.5 meq/100 g). CaCO<sub>3</sub> content presents no significant variation with depth but is higher in core 3 (average: 28%) and 4 (average: 15%). The lowest CaCO<sub>3</sub> values are observed in core 1 (average: 8%). The average water content by core can be sorted as follows: core 3 (37%) > core 4 (31%) > core 1 (28%) > core 2 (22%). While it presents

homogeneous vertical profiles in cores 1 and 2, the water content significantly decreases with depth in cores 3 (57%–26%) and 4 (46%–19%). SiO<sub>2</sub>, CaO and Fe<sub>2</sub>O<sub>3</sub> content appears stable with depth but presents significant variations between cores. The highest SiO<sub>2</sub> content is observed in cores 1 and 2 (> 78%). The lowest is notable in core 3 (57%), where Al<sub>2</sub>O<sub>3</sub> and CaO concentrations follow an inverse pattern (Al<sub>2</sub>O<sub>3</sub> > 4.2% and CaO > 15.2%). Fe<sub>2</sub>O<sub>3</sub> contents globally range from 1.9% and 3.0% except on core 1 (average: 1.1%).

TOC content shows little variation between cores (average value: 2%, standard deviation: 1%) and globally decreases with depth. The highest value is measured in the subsurface of core 3 (4.7%). Core 1 presents another pattern and remains relatively stable along the profile (from 2.3%–3.5%). The OI and HI records (Table S4 in the Supplement) present slight differences between the subsurface and the deepest layer of soil cores 2, 3 and 4 (HI values ranging from 152–335 mg HC g<sup>-1</sup> TOC, OI<sub>RE6</sub> values ranging from 154–218 mg O<sub>2</sub> g<sup>-1</sup> TOC). Cores 3 and 4 follow a relatively close trend with intermediate values of HI and higher values of OI<sub>RE6</sub>. Core 1 exhibits a similar pattern to core 2 for OI<sub>RE6</sub> but has the highest HI values. The calculation of hydrogen (HI) and oxygen (OI<sub>RE6</sub>) indexes (Table S4) allows for the approximation of the bulk chemistry of the soil organic matter (Espitalié et al., 1977; Vandenbroucke

**Table 2.** Physicochemical characteristics of the sampled cores. SD: standard deviation, –: no data. TOC: total organic carbon, CEC: cationic exchange capacity, LOI: loss on ignition at 1050 °C. Detection limits are available in Table S1. Station 1: park and green spaces; stations 2, 3 and 4: mesophilic grassland or deciduous planting trees.

Core	Depth (cm)	pH	Water content (%)	TOC (%)	CEC (meq/100 g)	CaCO <sub>3</sub> (%)	Clay (%)	Fine silt (%)	Coarse silt (%)	Sand (%)	LOI (%)	Na <sub>2</sub> O (%)	MgO (%)	Al <sub>2</sub> O <sub>3</sub> (%)	SiO <sub>2</sub> (%)	K <sub>2</sub> O (%)	CaO (%)	Fe <sub>2</sub> O <sub>3</sub> (%)
1	0–1	–	28	2.6	4.6	8	11	29	7	54	9	0.5	< 0.7	< 1.9	83	1.2	4.0	1.1
	1–2	–	31	3.1	5.1	–	–	–	–	–	11	< 0.5	< 0.7	< 1.9	81	1.2	4.0	1.1
	2–3	7.8	32	3.4	5.4	–	–	–	–	–	11	0.6	< 0.7	< 1.9	80	1.1	4.5	1.1
	3–4	–	32	3.5	5.5	–	–	–	–	–	11	0.5	< 0.7	< 1.9	81	1.1	4.2	1.1
	4–5	7.7	31	3.1	5.8	8	12	37	12	40	10	< 0.5	< 0.7	< 1.9	82	1.2	4.0	1.1
	5–6	–	29	2.9	5.6	–	–	–	–	–	10	0.7	< 0.7	< 1.9	81	1.1	4.0	1.1
	7–8	–	25	2.5	5.2	–	–	–	–	–	9	0.6	< 0.7	< 1.9	83	1.2	4.2	1.1
	9–10	7.7	24	2.3	5.7	9	9	27	6	58	9	< 0.5	< 0.7	< 1.9	82	1.3	4.5	1.2
	10–11	–	23	–	5.0	–	–	–	–	–	9	0.7	< 0.7	< 1.9	82	1.4	4.6	1.1
	Average		7.7	28	2.9	5.3	8	11	31	8	51	10	0.6	< 0.7	< 1.9	82	1.2	4.2
SD		0.04	4	0.4	0.4	1	1	5	3	10	1	0.1	–	–	1	0.1	0.3	0.0
2	0–1	7.4	29	2.5	4.8	11	16	41	12	31	11	0.6	< 0.7	2.2	76	1.3	6.4	1.9
	1–2	–	29	2.4	5.0	–	–	–	–	–	11	< 0.5	< 0.7	2.6	77	1.3	6.4	1.8
	2–3	–	28	2.2	4.8	–	–	–	–	–	10	< 0.5	< 0.7	2.6	76	1.5	6.7	1.9
	3–4	–	22	1.6	4.4	–	–	–	–	–	10	< 0.5	< 0.7	2.9	77	1.3	6.7	1.9
	4–5	7.8	20	1.3	3.8	12	17	34	12	38	9	< 0.5	< 0.7	2.8	78	1.2	6.7	1.9
	5–6	–	18	1.1	3.8	–	–	–	–	–	9	< 0.5	< 0.7	2.3	78	1.5	6.8	2.0
	7–8	–	18	1.0	3.6	–	–	–	–	–	9	< 0.5	< 0.7	2.9	74	1.2	6.7	1.9
	9–10	8.0	17	1.0	3.7	12	12	33	14	41	8	–	–	–	–	–	–	–
	10–11	–	16	–	3.5	–	–	–	–	–	8	0.5	< 0.7	2.4	79	1.3	6.9	2.0
	Average		7.7	22	1.7	4.2	12	15	36	13	36	9	0.6	< 0.7	2.6	77	1.3	6.7
SD		0.3	5	0.7	0.6	1	2	5	2	5	1	0.1	–	0.3	2	0.1	0.2	0.0
3	0–1	–	57	4.7	7.3	25	14	41	20	26	23	< 0.5	< 0.7	4.2	53	1.4	14.8	2.6
	1–2	7.5	49	4.1	7.2	–	–	–	–	–	21	< 0.5	< 0.7	4.5	57	1.4	16.8	2.8
	2–3	–	45	3.2	6.7	–	–	–	–	–	20	0.6	< 0.7	4.7	54	1.5	15.7	2.6
	3–4	–	40	2.7	6.2	–	–	–	–	–	19	0.6	< 0.7	4.1	55	1.4	16.1	2.7
	4–5	8.0	35	2.1	5.8	28	15	38	22	25	19	< 0.5	< 0.7	4.5	56	1.4	16.4	2.8
	5–6	–	31	1.7	5.4	–	–	–	–	–	18	0.5	< 0.7	4.2	54	1.5	16.4	2.7
	7–8	–	28	1.2	5.0	–	–	–	–	–	17	0.8	< 0.7	4.8	56	1.5	16.6	2.8
	9–10	8.0	26	1.1	4.8	30	16	42	18	24	17	0.5	< 0.7	5.6	56	1.4	16.8	2.7
	10–11	–	26	–	4.7	–	–	–	–	–	16	< 0.5	< 0.7	4.4	54	1.5	15.2	2.7
	Average		7.8	37	2.6	5.9	28	15	41	20	25	19	0.6	< 0.7	4.5	55	1.4	16.1
SD		0.3	11	1.3	1.0	3	1	2	2	1	2	0.1	–	0.5	1	0.1	0.7	0.1
4	0–1	–	46	3.3	6.8	15	19	54	19	8	15	< 0.5	< 0.7	4.2	66	1.4	9.6	2.6
	1–2	7.8	43	3.1	6.7	–	–	–	–	–	15	< 0.5	< 0.7	4.0	67	1.4	9.5	2.6
	2–3	–	40	2.7	6.5	–	–	–	–	–	14	0.6	< 0.7	4.1	66	1.3	9.6	2.6
	3–4	–	36	2.2	6.2	–	–	–	–	–	13	0.6	< 0.7	4.1	67	1.4	9.6	2.7
	4–5	7.8	31	1.6	5.7	15	16	48	23	13	13	0.5	< 0.7	4.2	68	1.6	10.2	2.7
	5–6	–	23	1.3	5.6	–	–	–	–	–	12	0.7	< 0.7	2.9	75	1.3	6.4	1.6
	7–8	–	22	1.1	5.3	–	–	–	–	–	12	< 0.5	< 0.7	4.7	69	1.4	10.2	2.7
	9–10	8.3	19	1.0	5.2	15	13	41	24	24	12	0.6	< 0.7	4.5	68	1.6	10.3	2.7
	10–11	–	19	–	5.2	–	–	–	–	–	11	0.5	< 0.7	4.7	68	1.6	10.1	2.8
	Average		8.0	31	2.0	5.9	15	16	48	22	15	13	0.6	< 0.7	4.2	68	1.5	9.5
SD		0.30	11	0.9	0.7	0	3	7	3	8	2	0.1	–	0.5	3	0.1	1.2	0.3
Total average		7.8	30	2.3	5.3	16	14	39	15	32	13	0.6	–	3.8	70	1.4	9.2	2.1
SD		0.2	10	1.0	1.0	8	3	8	6	15	4	0.1	–	0.9	11	0.1	4.6	0.7

and Largeau, 2007; Saenger et al., 2013). As each biological component (proteins, lignins, lipids, humic and fulvic acids, etc.) is characterized by a particular location within the van Krevelen diagram (H/C vs. O/C ratios) (Preston and Schmidt, 2006; Balaria et al., 2009; Falsone et al., 2012), the position of the studied samples in the pseudo van Krevelen diagram (HI : OI<sub>RE6</sub>) indicates their approximate bulk chemistry. Although HI and OI<sub>RE6</sub> values present slight heterogeneity, the distribution of points on the pseudo van Krevelen diagram reveals that the organic carbon detected in the four soil cores globally occurred as fulvic acids (Fig. 2) (Saenger et al., 2013).

### 3.1.2 Total and clayey mineralogical composition

Figure 3 presents the vertical profile of total and clayey mineralogical composition in the four soil cores (the complete data set is available in Table S5 in the Supplement). The study of total minerals indicates a dominance of quartz (> 50%) in all cores and no significant evolution of their composition downcore. Core 1 is characterized the highest quartz values (> 70%) and the lowest feldspar, calcite and mica concentration, with average concentrations of 3%, 4% and 9%, respectively. Core 3 exhibits different behavior, with the highest calcite and mica concentrations (22% and 20%) and lowest quartz and feldspar values (54% and 5%). A predominance of quartz is also observed at cores 2 and 4 (range: 67%–81%). The same proportions of calcite, mica and feldspar are measured in these two cores (averaging 10%, 12% and 4%, respectively). The clay minerals nature differed from core 1 to core 4 with an increasing percentage of smectite and a decreasing percentage of all the others (illite, kaolinite and chlorite). While illite dominates the assemblage of the clay minerals in cores 1 and 2 (> 41%), smectite is the preponderant clay mineral in cores 3 and 4 (> 50%). All the soil cores present higher smectite percentages with increasing depth (range: 34%–67%) and higher illite (32%–56%), kaolinite (14%–22%) and chlorite (9%–15%) percentages in the subsurface (< 3 cm).

The physicochemical parameters of soils (Table 2) support the AFES pedological classification of the upper soils of Gravelines as Thalassosols: the samples exhibit significant CaCO<sub>3</sub> contents and a predominantly loamy texture along the entire profile. This is consistent with the fine grain size (< 50 μm) typically observed in Thalassosols and in the plowed soils of the Wateringues marine plain (Sterckeman et al., 2004). In addition, CaCO<sub>3</sub> and CaO concentrations are highly correlated ( $R = 0.97$ ), suggesting a dominance of calcium and carbonates in these soils. This hypothesis is further supported by both the pH values, which reflect neutral to slightly basic conditions (Luo et al., 2015), and the global mineralogical composition of the studied soils.

### 3.1.3 Principal component analysis: pattern analysis of soil cores

The physicochemical parameters of soil samples revealed significant differences between the soil cores and depths. A principal component analysis (PCA) was performed on the physicochemical data set (Fig. 4). PCA showed that the two first principal components contributed to 78.4% of the total variance. The first principal component (PC1, 56.2%) is mainly formed by SiO<sub>2</sub>, Al<sub>2</sub>O<sub>3</sub>, CaO and Fe<sub>2</sub>O<sub>3</sub> contents and distinguishes soil cores based on their global mineralogical composition as previously described: sandy loam texture with a dominance of SiO<sub>2</sub> and quartz in cores 1 and 2 and silty loam texture with higher Al<sub>2</sub>O<sub>3</sub>, Fe<sub>2</sub>O<sub>3</sub> and CaO concentrations and clayey fractions in cores 3 and 4. Illite is dominant in cores 1 and 2, whereas smectite is the main clay mineral detected in cores 3 and 4. The second principal component (PC2, 22.2%), composed of TOC, water content and CEC, mostly separates subsurface samples from deep samples on cores 2, 3 and 4.

## 3.2 Vertical PTE concentrations in soil cores

### 3.2.1 Total PTE concentrations

PTE concentrations, measured along the four soil cores, are presented in Table 3. Results indicate variations in PTE concentrations between the studied cores and higher concentrations in some PTEs compared to the plowed soils of the so-called Wateringues marine plain (Sterckeman et al., 2004). Core 1 presents the lowest average concentrations for all the analyzed PTEs except Mo (0.4 mg kg<sup>-1</sup>). A significant vertical evolution is only observed for this element, increasing from 0.3 mg kg<sup>-1</sup> in the deepest layer to 0.5 mg kg<sup>-1</sup> in the subsurface. For the other cores, all the PTE concentrations are higher in the subsurface. Core 2 exhibits intermediate average values of 34, 257 and 10 mg kg<sup>-1</sup> for Cr, Mn and Ni, respectively. This core is also characterized by the highest average Cu concentrations (10 mg kg<sup>-1</sup>) and the lowest average Mo concentrations (0.3 mg kg<sup>-1</sup>). Core 3 is characterized by the highest average concentrations in Cr, Mn, Ni, Mo and Zn (with 57, 326, 17, 0.8 and 60 mg kg<sup>-1</sup>, respectively) and the lowest average concentrations in Cu (7 mg kg<sup>-1</sup>). Cr, Ni, Mo and Zn values are more than twice as high as the Wateringues marine plain background (Sterckeman et al., 2004) in the subsurface of this core. Finally, core 4 presents the same pattern as core 3 on average, but with slightly lower values. Values more than twice as high as the Wateringues marine plain background were observed only for Mo and Zn, which have concentrations higher than 0.3 and 71 mg kg<sup>-1</sup>, respectively.

### 3.2.2 PTE ratios of HCl leached fractions

Table 4 displays the leached fraction results for PTEs along depth for the four soil cores (concentrations and leached ra-

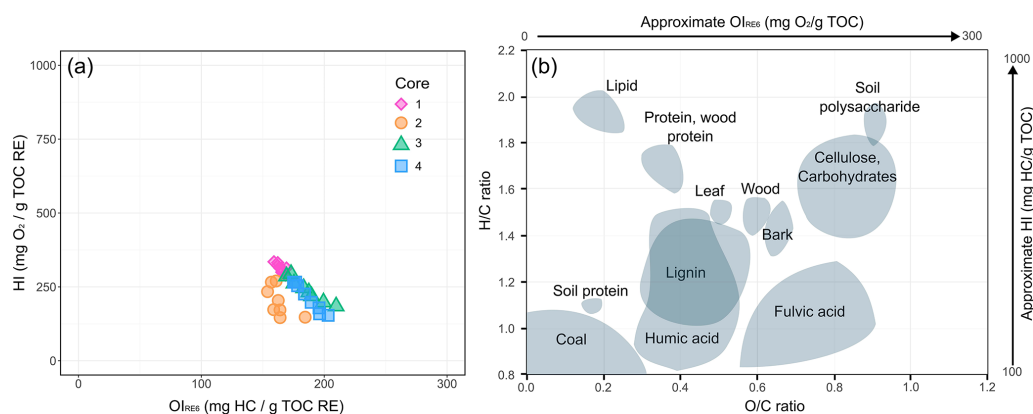


**Figure 2.** (a) Position of soil samples in the pseudo van Krevelen diagram (HI vs.  $OI_{RE6}$ ) according to the different soil cores. (b) location of soil molecules and biological compounds in the van Krevelen diagram (H/C vs. O/C) and approximate correspondence in the pseudo van Krevelen (Preston and Schmidt, 2006; Balaria et al., 2009; Falsone et al., 2012).

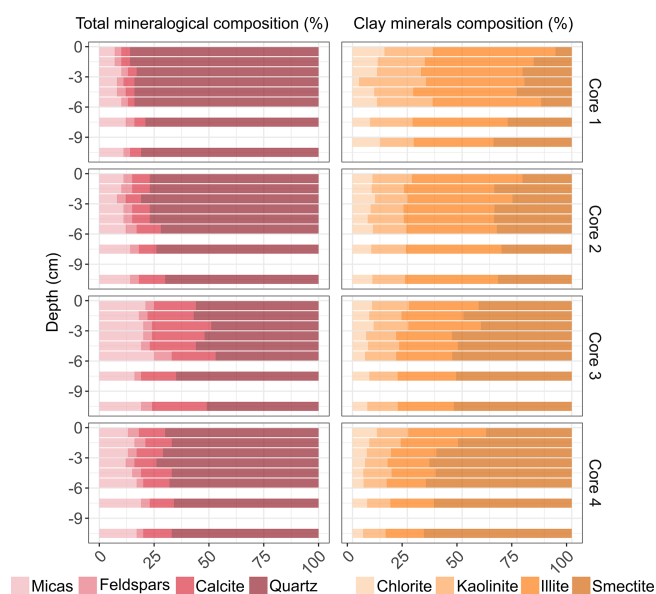


**Figure 3.** Vertical profiles of total (left) and clay (right) minerals on the four studied cores.

tios; leached/total in (%). The studied PTEs present different averages of leached ratios, increasing as follows: Cr (7 %), Mo (11 %), Ni (25 %), Zn (43 %), Cu (47 %), Mn (62 %) and Cd (68 %). For all the studied PTEs, the lowest leached ratios are calculated for core 3. An opposite trend is observed for core 2. Globally, the leached ratios of PTEs present no specific variation on the vertical profiles.

## 4 Discussion

### 4.1 Qualitative reactivity of soil cores toward PTEs

#### 4.1.1 Reactivity of organic matter in the studied soils

The results of the van Krevelen diagram (Fig. 2) suggest that the organic carbon detected in the studied soils is predominantly in the form of fulvic acids. This point may be explained by the presence of calcium carbonate in the studied soils, which is considered to stabilize lowly polymerized humic substances such as fulvic acids (Duchaufour, 1970; Duchaufour et al., 2020). This kind of humic substance is particularly soluble and has an adsorption capacity for metals that is 2–20 times higher than humic acids due to their greater amount of reactive functional groups (carboxyl, phenolic, carbonyl, etc.) (Donisa et al., 2003; Borůvka and Drábek, 2004; dos Santos et al., 2020). Furthermore, previous studies showed that pH values ranging from 6–8 tend to stabilize metal ions in soils by forming water-insoluble acid fulvic complexes (Schnitzer and Kerndorff, 1981; Boguta and Sokołowska, 2020). These results suggest a potential stabilization of PTE inputs by the organic matter of the studied soils, especially under the current acido-basic conditions (average pH value of 7.8). Thus, a significant change in the pH values could favor the mobilization of PTEs. While the organic carbon in the studied soils predominantly occurs as fulvic acids (without significant variations between cores and with depth), the pedological properties of the cores (Table 2) reveal notable differences that could influence their reactivity and the behavior of their absorbent complex.

#### 4.1.2 Discrimination of cores by the reactivity of their absorbent complex

The results of the PCA (Fig. 4) reveal that the soil cores and depths can be distinguished between by their mineralogical composition (PC1) and physicochemical properties

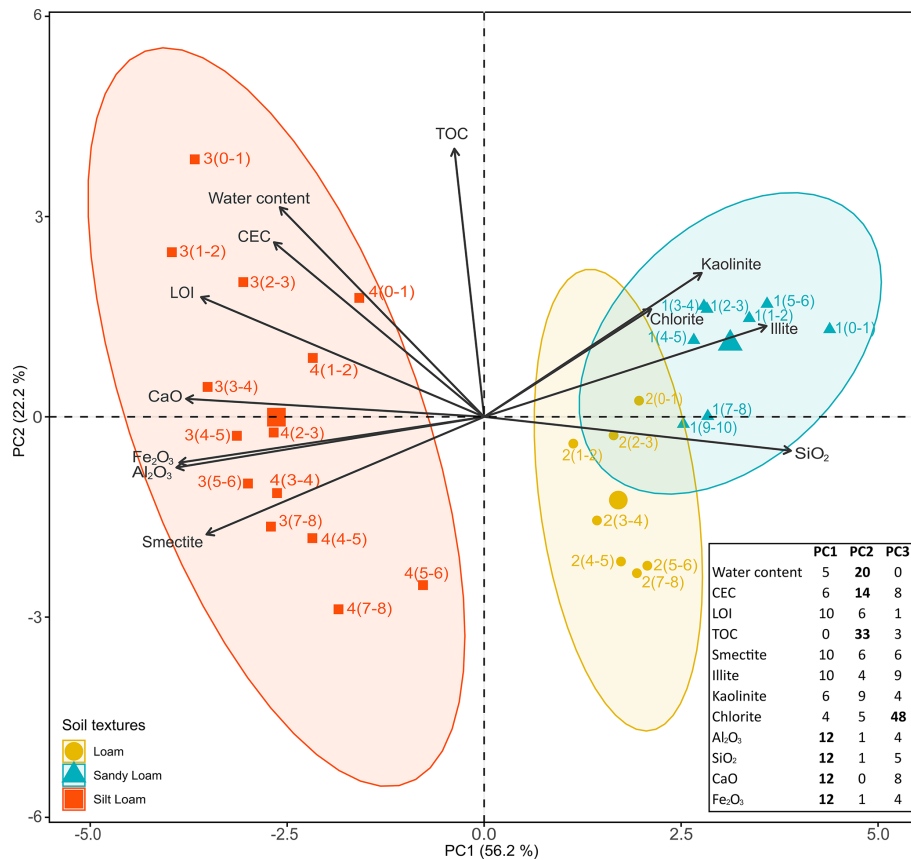


**Figure 4.** Principal component analysis (PCA) illustrating the variations in the pedological variables (arrows) for all the soil cores from Gravelines city and textures (colored symbols). Three domains (ellipses) correspond to the different textures of soils and highlight distinct cores, depths and behaviors. Larger symbols indicate the centroid of values for each soil texture. The percentage of contribution of the different pedological variables in the building of the PCA axis is inset (bottom right). The most important contributors are denoted in bold.

(PC2), which may influence their capacity to retain metallic contaminants and thus their fate in the environment (Fijałkowski et al., 2012; Campillo-Cora et al., 2020; Yu et al., 2023). Focusing on the first principal component, previous studies highlighted the importance of smectite in soil absorption capacities (Varadachari et al., 1994; Hanna et al., 2009; Orucoglu et al., 2022) due to their specific surface area and their influence on CEC values (Otinola and Oloade, 2020). This observation is consistent with the higher proportion of smectite detected in cores 3 and 4, presenting a higher sorption capacity than cores 1 and 2. The second principal component describes the sorption efficiency of the clay–humus soil complex through organic compounds and the presence of fine-grained materials (Warwick et al., 1998; Bronick and Lal, 2005; Hernandez-Soriano and Jimenez-Lopez, 2012). This component mostly discerns subsurface samples from deep samples in cores 2, 3 and 4, reflecting the enhanced retention capacity of contaminants near the soil surfaces (Fiedler et al., 2007; Chitolina et al., 2020). By combining the two principal components, the PCA differentiates between the soil cores and depths based on the

potential retention capacity of their absorbent complex (Impellitteri et al., 2002; Bradl, 2004; Lasota et al., 2020). The subsurface samples of cores 3 and 4 (nearest to the industrial emitters) present the highest sorption capacities compared to the deeper ones. Core 2 (intermediate location between industries and city center) presents the same pattern but with a globally lower sorption capacity than cores 3 and 4. Core 1 (in the city center) exhibits the lowest sorption capacities with a notable homogeneity with depth.

#### 4.2 Soil contaminations by industrial or urban PTE inputs

##### 4.2.1 Highlighting atmospheric PTE inputs in the soils of Gravelines

Enrichment factors (EFs) were calculated for Cr, Mn, Ni, Cu, Zn, Mo and Cd by comparing the soils of Gravelines to those of the surrounding Wateringues marine plain and normalizing to Al contents (Fig. 5). Core 1 was not considered because of its Al concentrations being below the detection limit. According to Chen et al. (2007), cores 2, 3 and 4 can be

**Table 3.** Evolution of PTE contents with depths of the four soil cores collected in Gravelines ( $\text{mg kg}^{-1}$ ). Values more than twice higher than the Wateringues marine plain background (median values) are denoted in bold. SD: standard deviation. N.d.: not determined; “–” means no data.

Core	Depth (cm)	Cr	Mn	Ni	Cu	Zn	Mo	Cd
1	0–1	22	102	8	7	39	<b>0.5</b>	0.16
	1–2	22	103	8	8	41	<b>0.5</b>	0.16
	2–3	24	109	8	8	45	<b>0.5</b>	0.17
	3–4	22	107	8	8	<b>72</b>	<b>0.4</b>	0.19
	4–5	22	103	8	8	44	<b>0.4</b>	0.17
	5–6	21	105	8	8	41	<b>0.4</b>	0.18
	7–8	21	105	8	8	41	0.3	0.20
	9–10	–	–	–	–	–	–	–
	10–11	24	106	8	8	40	0.3	0.18
Average		22	105	8	8	45	0.4	0.18
SD		1	2	0.2	0.3	10	0.1	0.01
2	0–1	37	278	11	11	67	<b>0.6</b>	0.39
	1–2	36	265	11	10	63	<b>0.5</b>	0.34
	2–3	30	276	10	11	63	0.2	0.33
	3–4	33	250	10	12	64	0.2	0.33
	4–5	34	254	10	11	56	0.2	0.31
	5–6	35	255	10	9	54	0.3	0.34
	7–8	33	240	10	9	55	0.2	0.32
	9–10	–	–	–	–	–	–	–
	10–11	33	240	9	9	47	0.2	0.33
Average		34	257	10	10	59	0.3	0.34
SD		2	14	0.5	1	6	0.1	0.02
3	0–1	<b>67</b>	381	<b>22</b>	9	<b>90</b>	<b>1.4</b>	0.42
	1–2	<b>63</b>	335	<b>19</b>	8	<b>73</b>	<b>0.9</b>	0.42
	2–3	<b>60</b>	333	<b>18</b>	8	68	<b>0.9</b>	0.40
	3–4	<b>57</b>	322	17	8	58	<b>0.7</b>	0.39
	4–5	<b>57</b>	321	16	7	53	<b>0.7</b>	0.38
	5–6	55	308	16	7	50	<b>0.6</b>	0.33
	7–8	52	299	15	7	47	<b>0.6</b>	0.34
	9–10	–	–	–	–	–	–	–
	10–11	49	308	14	6	45	<b>0.4</b>	0.30
Average		57	326	17	7	60	0.8	0.37
SD		5	24	2	1	14	0.3	0.04
4	0–1	42	300	13	9	56	<b>0.6</b>	0.24
	1–2	41	281	13	9	<b>77</b>	<b>0.6</b>	0.23
	2–3	41	282	12	9	47	<b>0.5</b>	0.24
	3–4	41	292	12	9	45	<b>0.4</b>	0.23
	4–5	45	292	12	9	43	<b>0.4</b>	0.23
	5–6	40	290	12	9	43	0.3	0.21
	7–8	38	279	11	8	40	0.3	0.21
	9–10	–	–	–	–	–	–	–
	10–11	38	274	12	8	40	0.2	0.20
Average		41	286	12	9	49	0.4	0.22
SD		2	8	0.5	0.5	11	0.1	0.01
Total average		39	244	12	9	53	0.5	0.28
SD		13	86	4	1	13	0.3	0.09
Wateringues marine plain background <sup>a</sup>		28	207	9	7	36	0.2	0.24

<sup>a</sup> Sterckeman et al. (2004).

**Table 4.** Leached concentrations ( $\text{mg kg}^{-1}$ ) and leached ratios (leached concentration/total concentration in %) of the studied PTEs in the four soil cores, after 1 M HCl extraction. SD: standard deviation, n.d.: not determined, -: no data.

Core	Depth (cm)	Leached concentrations ( $\text{mg kg}^{-1}$ )							Leached ratios (%)						
		Cr	Mn	Ni	Cu	Zn	Mo	Cd	Cr	Mn	Ni	Cu	Zn	Mo	Cd
1	0–1	2	60	2	4	21	0.05	0.12	8	59	28	51	54	11	75
	1–2	2	67	2	4	23	0.04	0.12	8	64	28	53	56	9	75
	2–3	2	68	2	4	23	0.04	0.13	7	62	27	52	52	8	76
	3–4	2	68	2	4	25	0.04	0.14	7	63	28	52	–	9	74
	4–5	2	64	2	4	23	0.03	0.14	7	62	28	51	52	7	82
	5–6	2	64	2	4	22	0.03	0.13	7	61	27	53	54	8	72
	7–8	2	65	2	4	22	0.03	0.13	8	61	28	53	53	10	65
	9–10	–	–	–	–	–	–	–	–	–	–	–	–	–	–
	10–11	2	60	2	4	20	0.02	0.13	6	56	25	52	49	6	72
	Average		2	64	2	4	22	0.04	0.13	7	61	27	52	53	8
SD		0	3	0	0	1	0.01	0.01	1	2	1	1	2	1	5
2	0–1	3	166	3	6	35	0.07	0.26	8	60	25	53	52	13	67
	1–2	3	163	3	6	34	0.07	0.24	9	62	26	54	54	15	71
	2–3	3	167	3	6	33	0.06	0.24	11	60	26	54	51	29	73
	3–4	4	163	3	6	34	0.04	0.22	11	65	28	53	53	17	67
	4–5	3	160	3	6	27	0.04	0.21	10	63	26	54	49	24	68
	5–6	3	151	3	5	25	0.03	0.21	9	59	26	52	46	12	62
	7–8	3	161	3	5	27	0.03	0.22	10	67	27	55	50	14	69
	9–10	–	–	–	–	–	–	–	–	–	–	–	–	–	–
	10–11	3	154	3	5	23	0.03	0.21	10	64	27	56	49	14	64
	Average		3	161	3	6	30	0.05	0.23	10	63	26	54	50	17
SD		0	5	0	0	4	0.02	0.02	1	3	1	1	2	6	3
3	0–1	4	222	5	4	43	0.14	0.26	6	58	21	41	48	10	62
	1–2	4	208	4	4	35	0.09	0.26	6	62	23	43	48	10	62
	2–3	3	192	3	3	27	0.09	0.24	5	58	19	38	40	11	60
	3–4	3	196	3	3	22	0.08	0.23	5	61	19	40	39	11	59
	4–5	3	195	3	3	20	0.08	0.22	6	61	21	40	38	12	58
	5–6	3	186	3	3	17	0.06	0.20	5	60	19	39	34	10	61
	7–8	3	178	3	3	15	0.06	0.20	6	60	19	38	32	10	59
	9–10	–	–	–	–	–	–	–	–	–	–	–	–	–	–
	10–11	3	177	3	2	14	0.06	0.18	6	58	20	35	31	14	60
	Average		3	194	3	3	24	0.08	0.22	6	60	20	39	39	11
SD		0	14	1	0	10	0.02	0.03	0	2	1	2	6	1	1
4	0–1	3	191	4	4	22	0.05	0.17	7	64	30	43	39	8	71
	1–2	3	178	4	4	20	0.05	0.17	7	63	28	42	26	8	74
	2–3	3	178	3	4	17	0.04	0.17	7	63	27	41	37	8	71
	3–4	3	179	3	4	16	0.03	0.16	7	61	27	43	36	7	70
	4–5	3	186	3	4	14	0.03	0.15	6	64	27	42	33	8	65
	5–6	3	177	3	4	13	0.03	0.15	7	61	25	40	31	10	71
	7–8	3	175	3	3	13	0.02	0.14	7	63	26	41	32	7	67
	9–10	–	–	–	–	–	–	–	–	–	–	–	–	–	–
	10–11	3	178	3	3	13	0.01	0.15	8	65	26	38	33	4	75
	Average		3	180	3	4	16	0.03	0.16	7	63	27	41	35	8
SD		0	5	0	0	3	0.01	0.01	0	1	2	1	3	2	3
Total average		3	150	3	4	23	0.05	0.18	7	62	25	47	44	11	68
SD		1	52	1	1	8	0.03	0.05	2	2	3	7	9	5	6

globally described by minor PTE enrichments ( $1 < EF < 3$ ; Fig. 5) except for Mo (punctual moderately severe enrichments, with  $5 < EF < 10$ ). As suggested in a previous study (Casetta et al., 2024), the present PTE values and EFs support the hypothesis of a diffuse contamination of the soils of Gravelines. Furthermore, vertical profiles of enrichment factors show that the slight PTE accumulations in cores 2 (Cr, Mn, Ni, Cu, Zn, Mo and Cd), 3 (Cr, Ni, Zn and Mo) and 4 (Zn and Mo) mostly occur within the first 2 cm. As reported in numerous studies (Williams et al., 1987; Li and Shuman, 1996; Sterckeman et al., 2000), these patterns of superficial accumulation suggest atmospheric and anthropogenic PTE inputs, particularly in cores 2 and 3.

#### 4.2.2 Are the PTE inputs in stations 2 and 3 related to industrial dust?

The previous characterization of dust fallout collected in Gravelines revealed high enrichment in some PTEs compared to the upper continental crust and using Sc as an immobile element (Taylor and McLennan, 1995):  $EF(Cr) = 108$ ,  $EF(Mn) = 36$ ,  $EF(Ni) = 78$ ,  $EF(Zn) = 60$ ,  $EF(Mo) = 169$ ,  $EF(Cd) = 235$  (Casetta et al., 2024). As Cu (with  $EF < 20$ ) may originate from multiple sources in such an urban environment (roof, garden and lawn treatment, and car brakes; Panagos et al., 2018), it is be used to trace industrial inputs. Considering these results and other studies carried out using the atmospheric particles emitted in the Dunkerque agglomeration (Alleman et al., 2010; Hleis et al., 2013; Kfoury et al., 2016), a metallurgical dust influence could explain the chemical signatures of the soil cores 2 and 3 from two points of view: (1) the slight but notable accumulation of Mo, Cr and Ni in the subsurface of soil cores 2 and 3 and (2) the same pattern of accumulation of Mn, Zn and Cd, three other PTEs associated with industrial activities. For core 3, this hypothesis is also supported by the strong correlations calculated between its Mo, Cr and Ni enrichment factors ( $R > 0.93$ ) and its Mn, Cd and Zn enrichment factors ( $R > 0.81$ ). In contrast, these correlations are significantly lower for the core 2. This trend of high correlations between the studied PTEs (e.g.,  $R > 0.97$  for Cr and Ni EFs) is globally observed for the whole data set (Table 5). Based on this interpretation and the calculated EFs (Fig. 5), both cores seem to be influenced by Cr, Ni and Mo inputs, but core 2 appears to be more impacted by Mn, Zn and Cd inputs than core 3. Considering Cr as the less mobile PTEs in the studied soils (Table 4), the use of some PTEs against Cr ratios ( $Zn / Cr$  vs.  $100 Cd / Cr$  and  $Cr / Mo$  vs.  $Ni / Mo$ , Fig. 6) allowed us to visualize and highlight these two different anthropogenic signatures in the considered soil cores, according to depth. Thus, core 3 samples present a chemical signature close to the studied dust data (Fig. 6a). The signature is different for core 2 samples, with the highest considered PTE ratios.  $Cr / Mo$  and  $Ni / Mo$  ratios (Fig. 6b) underline that the core 2 subsurface samples are marked by the chemical signature highlighted in core 3.

Knowing the diversity of atmospheric emissions from metallurgical activities in the studied area (Alleman et al., 2010; Hleis et al., 2013; Géorisques, 2023a, b), the presence of different industrial chemical signatures in soils is not surprising.

No statistically significant correlation was observed between the calculated EFs and the distance from the emission sources, as previously observed with more topsoil samples in Gravelines (Casetta et al., 2024). According to this latter study and regarding the spatial location of the current soil cores, the highest EFs measured on core 2 seem to be mostly related to the soil exposure, i.e., the absence of vegetal or urban protecting barriers. Concerning Mn, Cu, Zn and Cd concentrations, urban influences in soils cannot be excluded, considering the potential emission of Mn, Cu and Zn by non-exhaust road traffic (Smolders and Degryse, 2002; Lee et al., 2006; Guo et al., 2012) as well as the correlation between their enrichment factors in soils ( $R = 0.81$ ; Table 5). Likewise, the use of Cu and Cd as pesticides or Mn and Cd occurrence in fertilizers and compost (Baize, 1997; Campos, 2003; He et al., 2005) remain possible.

#### 4.3 Mobility of PTEs in the soils of Gravelines

Assessing the impact of industrial dust on the environment partly stands on the mobility of their dust-borne metals in soils. Thus, the general mobility of PTEs in contaminated soils (particularly cores 2 and 3) was estimated using 1 M HCl single extraction. As it is easy to manage, this kind of extraction is often performed on different types of sediment (Hamdoun et al., 2015; Yu et al., 2021) in order to assess the bio-accessible fraction of a specific metal content (Snape et al., 2004; Philippe et al., 2008; Roosa et al., 2016). HCl is prone to extracting the labile fraction (exchangeable, bound to calcium carbonate, part of oxides and acid volatile sulfides) (Billon, 2001; Townsend et al., 2007; Waterlot et al., 2017; Pelfrène et al., 2020). Considering the studied soils, particularly rich in calcium carbonates (12 %–30 %), the use of 1 M HCl with a prolonged reaction time was required to avoid underestimating the buffering effect of carbonates as described in the methodology. Based on these considerations, this HCl extraction highlights the mobility of specific PTEs under local pH changes. Literature data summarized in Table 1 show that a high mobility for Cu, Mn, Mo, Ni, Zn and to a lesser extent Cd and a low mobility for Cr can be expected after 1 M HCl leaching of the studied soils

##### 4.3.1 Comparison of the different stations

As observed for PTE concentrations, no significant evolution in PTE leached ratios (leached/total content) was observed in the vertical profiles of the four soil cores (according to their SD values) (Table 4). Moreover, PTE leached ratios remain stable even at the subsurface despite the occurrence of organic matter. These results are consistent with the observed lack of correlation between the PTE leached fractions and



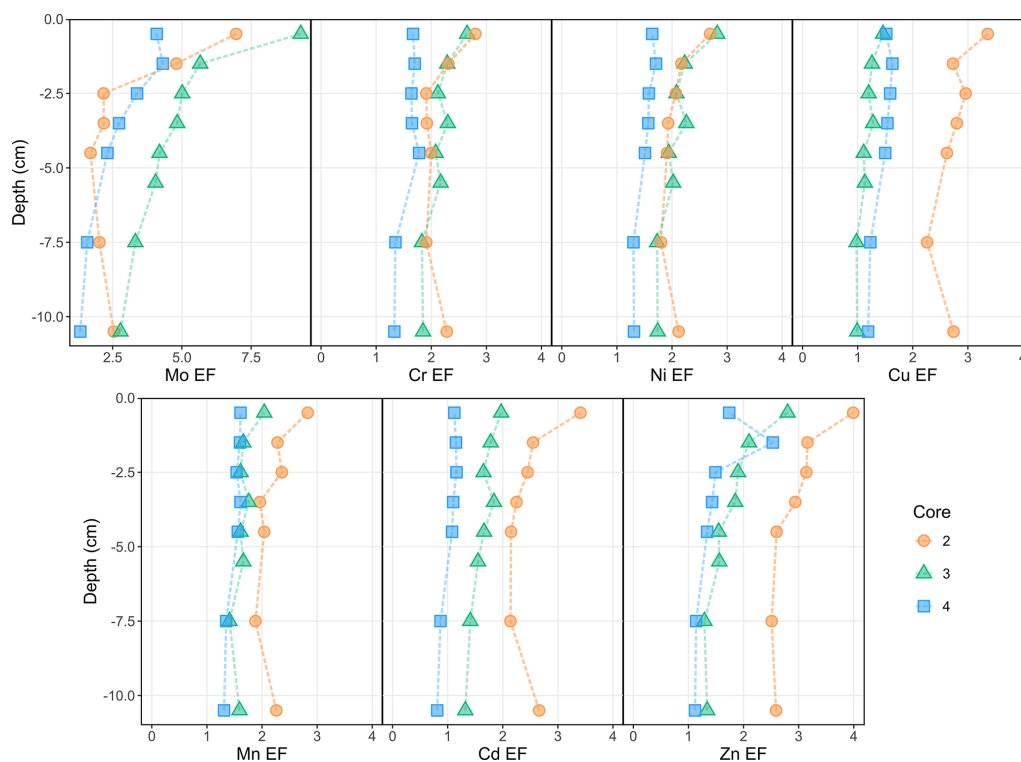


**Figure 5.** Vertical profiles of Cr, Mn, Ni, Cu, Zn, Mo and Cd enrichment factors (against Al) in cores 2, 3 and 4. Reference materials correspond to the median values obtained on the Wateringues marine plain soils (Sterckeman et al., 2004).

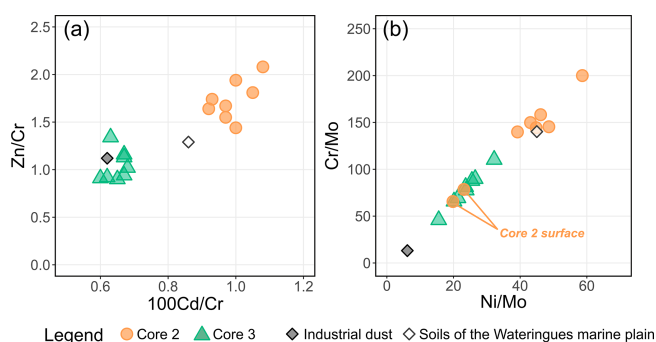


**Figure 6.** Elemental ratio diagrams for cores 2 and 3, industrial bulk dust and median Wateringues maritime plain soils. (a) Zn / Cr vs. 100 Cd / Cr and (b) Cr / Mo vs. Ni / Mo.

TOC contents (Table 5). The soil core collected in station 1 (city center) is characterized by the less efficient absorbent complex (Fig. 4) and the lowest total PTE concentrations (Table 3). However, Cu, Zn and Cd (known to be more mobile when coming from mixed anthropogenic sources; Baize, 1997) were the most extracted PTEs at this station (Table 4). Thus, these results reveal a classical urban PTE contamination in the city center (station 1). The soil core collected at station 4 presents higher absorbent capacities (Fig. 4) and higher PTE total concentrations in Cr, Mn, Ni and Mo com-

pared to the soil cores 1 and 2 (Table 3). The correlation between total PTE concentrations may reflect an industrial signature (Cr, Mn, Ni and Mo) on these soils despite the relatively low PTE EFs (Fig. 5). Compared to the other cores, the leached ratios are average for Cr, Mn and Ni and slightly lower for Cu, Zn and Mo (Table 4). This could be related to (1) the soil properties (rich in clay fraction), (2) relatively lower solubility of PTEs from industrial dust or (3) both. The important Cd leached fraction (70 %) is, however, noticeable (Table 4). This result is of concern regarding the presence of allotment gardens close to station 4. The highest PTE EFs, in particular at the surface, are measured in the soil cores 2 and 3 (Fig. 5). The superficial PTE accumulations on these stations (located close to the industrial emitters) were previously related to industrial and atmospheric inputs (see Sect. 4.2.2). As the present study aims to discuss the ecotoxicological impact of industrial dust deposition on urban soils, the following parts focus on the PTE leached ratios in these cores 2 and 3.

#### 4.3.2 Mobility of all the studied PTEs in cores 2 and 3

In the soil cores 2 and 3, Mn, Cu, Zn and Cd appear rather mobile compared to Cr, Ni and Mo (Table 4). The mobility of the first group of elements (average leached values both > 39 %) in the presence of 1 M HCl is not surprising considering their natural mobility in oxidant and/or acidic

conditions (Table 1). The high mobility of Mn and Cd (average leached values > 60%) can be additionally explained by (1) their natural association to the exchangeable and calcium carbonates fractions in soils (Table 1, Ren et al., 2015; Kubier et al., 2019) and (2) the concentration of carbonate calcium (easily dissolved by 1 M HCl) in these soils (ranging 12%–28%). Concerning the second group of elements, low Cr leached ratios are consistent with the natural behavior of this PTE in soils (Table 1) and may indicate the association of this element with anthropogenic or natural refractory phases (Fendorf, 1995). Ni and Mo naturally present strong affinities with calcium carbonates, organic matter and Fe/Mn oxides (Shi et al., 2012; Bielefeldt and Vos, 2014; King et al., 2018). They are expected to be particularly mobile under oxidant and acidic conditions (Table 1). Despite the use of 1 M HCl treatment, the moderately low Ni and Mo leached ratios (< 27% for Ni and < 17% for Mo) suggest their association with anthropogenic or natural (iron oxides and silicates) refractory phases (specific adsorption on organic matter or inclusion in mineralogical phases) (Bibak et al., 1994; Goldberg et al., 1996; Gardner et al., 2012; Barman et al., 2015).

#### 4.3.3 Specific mobility of industrial dust-borne PTEs in cores 2 and 3

The four dominant types of industrial dust fallout identified in the city of Gravelines (coal particles, slags, iron ores and aluminum oxides) are the main bearing phases of several PTEs, including Cr, Ni, Mo, Zn, Cd and Mn (Casetta et al., 2024). In light of current knowledge, it is not possible to relate a PTE to a specific bearing phase. As Cr, Ni and Mo are supposed to be present in soils within refractory phases, the hypothesis of an industrial nature of these latter in cores 2 and 3 is supported by (1) the previously described Cr, Ni and Mo enrichment factors and (2) the known low mobility of Cr and Ni found in industrial coals and slags (Cabrera-Real et al., 2012; Albertsson et al., 2014; Mombelli et al., 2016; Zhao et al., 2018; Feng et al., 2000). The high mobility of Mn, Zn and Cd in cores 2 and 3 is consistent with previous studies focused on their mobility in industrial coals and slags (Fernández-Turiel et al., 1994; Querol et al., 1995; Han et al., 2019; Li et al., 2020; Kicińska, 2021). Regarding the absence of significant correlations between the Mn and Cd EFs and their leached ratios, it is, however, complicated to draw conclusion about their origin, chemical form and subsequent behavior in the soil cores. Only Zn presents a positive correlation between total content and leached ratios ( $R = 0.78$ ), suggesting the higher mobility of this element from anthropogenic inputs.

Thus, the study tends to reveal the stability of industrial dust bearing Cr, Ni and Mo in soils, as these PTEs were lowly leached despite the use of a powerful extraction reagent (1 M HCl). These results highlight a relative immobility of these harmful elements in the environment (Smedley and Kiniburgh, 2017; DesMarais and Costa, 2019) and then their

low bioavailability. Nevertheless, this stability does not eliminate the potential environmental and sanitary risks. The accumulation of these PTEs in the soil subsurface layer, combined with changes in environmental conditions such as pH or redox potential, could increase their mobility. As the studied soils latter are developed at low altitude (0–25 m), their vulnerability in the context of ongoing sea level rise is particularly significant. Flooding events, which could become more frequent due to rising sea levels, could affect soil salinity and redox conditions, potentially releasing these stable contaminants into the environment (Hailegnaw et al., 2024; Pellegrini et al., 2024). Additionally, the use of these soils for allotment gardens near industrial emitters poses a risk of human exposure to contaminants through the cultivation of vegetables or soil contact, especially for children (Calabrese et al., 1997; Crispo et al., 2021). Thus, while our results suggest limited immediate mobility of Cr, Ni, and Mo, a monitoring of environmental changes and their effects on these PTEs is recommended for assessing long-term environmental and sanitary risks.

## 5 Conclusion

The main challenge of this study was to evaluate the vertical distribution and mobility of PTEs in the soils of Gravelines, which are mainly derived from the deposition of industrial dusts. Although the studied soils globally present minor PTE enrichments, specific levels of contamination were identified in the soil cores. These were related to industrial dust deposition through (1) the higher PTE concentrations and EFs in the core subsurface (0–3 cm), suggesting anthropogenic and atmospheric inputs of the contaminants, and (2) the significant associations of metallurgical tracer elements, as Cr, Ni and Mo or Mn, Zn and Cd. The assessment of the general mobility of industrial PTEs in soils reveals the stability of Cr, Ni and Mo despite the use of a relatively strong extractant (1 M HCl) and suggests their association to industrial refractory phases such as coals and slags. Conversely, Mn, Zn and Cd have a higher mobility. Knowing that 1 M HCl extraction destabilizes the exchangeable, carbonated, organic and oxide soil fractions, these PTEs could not be only related to metallurgical particles.

The calcareous soils of Gravelines globally present low absorbent capacities, partially counterbalanced by their buffering capacities. In the case of destabilization of industrial dust in soils, these results highlight that the released ions (especially Cr, Ni and Mo) would be more retained in soils with more efficient absorbent complex and significant carbonate contents (e.g., core 3 vs. core 2). Then, the present study shows the importance of studying pedological parameters (texture, mineralogy, TOC, water content and CEC) to understand their influence on the PTE concentrations and to evaluate their mobility. In the future, however, interactions between soil and other environmental compartments are likely

to be disrupted by climate change. This could increase particle weathering (e.g., carbonate, oxides) and consequently induce higher mobility of some PTEs (Hailegnaw et al., 2024; Pellegrini et al., 2024). This hypothesis must be particularly considered, regarding (1) the potential toxicity of these elements in their mobile form; (2) their accumulation in the soil subsurface, which interacts with all the environmental compartments; and (3) the possible PTE contamination of food produced in the urban allotment gardens (near the industrial emitters) and consumed by local inhabitants.

**Code and data availability.** All the data used in this study are presented in the tables and the Supplement.

**Supplement.** The supplement related to this article is available online at <https://doi.org/10.5194/soil-11-467-2025-supplement>.

**Author contributions.** MC: conceptualization, data curation, formal analysis, investigation, methodology, validation, visualization writing (original draft preparation), writing (review and editing); SP: conceptualization, funding acquisition, investigation, methodology, project administration, resources, supervision, validation, writing (review and editing); LC: conceptualization, investigation, methodology, supervision, validation, writing (review and editing); DD: investigation, validation, writing (review and editing); GB: validation, writing (review and editing); FB: investigation, validation, writing (review and editing); FH: investigation, resources, validation, writing (review and editing); MH: resources, supervision, writing (review and editing); JC: conceptualization, funding acquisition, investigation, methodology, project administration, resources, supervision, validation, writing (review and editing).

**Competing interests.** The contact author has declared that none of the authors has any competing interests.

**Disclaimer.** Publisher's note: Copernicus Publications remains neutral with regard to jurisdictional claims made in the text, published maps, institutional affiliations, or any other geographical representation in this paper. While Copernicus Publications makes every effort to include appropriate place names, the final responsibility lies with the authors.

**Acknowledgements.** The authors would like to thank the agglomeration of Dunkerque, the city of Gravelines, and the DREAL, SPPPI and ALOATEC organizations for their support. ICP-AES/MS and XRD analyses were performed using the Chevreul Institute Platform (ULille/CNRS) and the Platform CARMIN – ULille infrastructure, respectively. We also thank Véronique Alaimo and Marion Delattre for their technical support and assistance with these analyses. Laurine Hopf and Louise Legrand are gratefully acknowledged for their helpful technical assistance in the laboratory during their training. Finally, we thank the three review-

ers for their constructive comments, which helped improve the quality of the paper.

**Financial support.** This research was supported by the Pôle Métropolitain Côte d'Opale (PMCO) and the Hauts-de-France Region through a PhD scholarship (2020–2023). This work has been financially supported by the European Union (ERDF), the French State, the French Region Hauts-de-France and Ifremer, in the framework of the CPER MARCO and CPER Climibio programs (2015–2021). The study also received support from the INSU CNRS program (AO EC2CO (HYBIGE) 2023–2024) and the SFR Campus de la Mer (AAP SFR 2022-2).

**Review statement.** This paper was edited by Maria Jesus Gutierrez Gines and reviewed by Thomas Chalaux-Clergue, Andrew Hursthouse, and one anonymous referee.

## References

- Albertsson, G. J., Engström, F., and Teng, L.: Effect of the Heat Treatment on the Chromium Partition in Cr-Containing Industrial and Synthetic Slags, *Steel Res. Int.*, 85, 1418–1431, <https://doi.org/10.1002/srin.201300231>, 2014.
- Alleman, L. Y., Lamaison, L., Perdrix, E., Robache, A., and Galloo, J.-C.: PM<sub>10</sub> metal concentrations and source identification using positive matrix factorization and wind sectoring in a French industrial zone, *Atmos. Res.*, 96, 612–625, <https://doi.org/10.1016/j.atmosres.2010.02.008>, 2010.
- Amar, M., Benzerzour, M., Kleib, J., and Abriak, N.-E.: From dredged sediment to supplementary cementitious material: characterization, treatment, and reuse, *Int. J. Sediment Res.*, 36, 92–109, <https://doi.org/10.1016/j.ijsrc.2020.06.002>, 2021.
- Aran, D., Maul, A., and Masfarau, J.-F.: A spectrophotometric measurement of soil cation exchange capacity based on cobalthexamine chloride absorbance, *CR Geosci.*, 340, 865–871, <https://doi.org/10.1016/j.crte.2008.07.015>, 2008.
- Baize, D.: *Teneurs totales en éléments traces métalliques dans les sols (France)*, INRA Editions, Paris, 408 pp., ISBN 978-2-7380-0747-6, 1997.
- Baize, D. and Girard, M.-C.: *Référentiel pédologique*, [Éd.] 2008, Éd. Quae, Versailles, ISBN 978-2-7592-0185-3, 2009.
- Balaria, A., Johnson, C. E., and Xu, Z.: Molecular-Scale Characterization of Hot-Water-Extractable Organic Matter in Organic Horizons of a Forest Soil, *Soil Sci. Soc. Am. J.*, 73, 812–821, <https://doi.org/10.2136/sssaj2008.0075>, 2009.
- Barman, M., Datta, S. P., Rattan, R. K., and Meena, M. C.: Chemical fractions and bioavailability of nickel in alluvial soils, *Plant Soil Environ.*, 61, 17–22, <https://doi.org/10.17221/613/2014-PSE>, 2015.
- Bibak, A., Møberg, J. P., and Borggaard, O. K.: Content and Distribution of Cobalt, Copper, Manganese and Molybdenum in Danish Spodosols and Ultisols, *Acta Agr. Scand. B-S. P.*, 44, 208–213, <https://doi.org/10.1080/09064719409410247>, 1994.
- Bielefeldt, A. R. and Vos, C.: Stability of biologically reduced chromium in soil, *J. Environ. Chem. Eng.*, 2, 550–556, <https://doi.org/10.1016/j.jece.2013.10.012>, 2014.

- Billon, G.: Géochimie des métaux et du soufre dans les sédiments des estuaires de la Seine et de l'Authie, Thèse de doctorat, Lille 1, <https://scirp.org/reference/referencespapers?referenceid=3171390> (last access: 17 March 2022), 2001.
- Birch, G. F.: Determination of sediment metal background concentrations and enrichment in marine environments – A critical review, *Sci. Total Environ.*, 580, 813–831, <https://doi.org/10.1016/j.scitotenv.2016.12.028>, 2017.
- Boguta, P. and Sokolowska, Z.: Zinc Binding to Fulvic acids: Assessing the Impact of pH, Metal Concentrations and Chemical Properties of Fulvic Acids on the Mechanism and Stability of Formed Soluble Complexes, *Molecules*, 25, 1297, <https://doi.org/10.3390/molecules25061297>, 2020.
- Borůvka, L. and Drábek, O.: Heavy metal distribution between fractions of humic substances in heavily polluted soils, *Plant Soil Environ.*, 50, 339–345, <https://doi.org/10.17221/4041-PSE>, 2004.
- Bout-Roumazeilles, V., Cortijo, E., Labeyrie, L., and Debrabant, P.: Clay mineral evidence of nepheloid layer contributions to the Heinrich layers in the northwest Atlantic, *Palaeogeogr. Palaeoclimatol.*, 146, 211–228, [https://doi.org/10.1016/S0031-0182\(98\)00137-0](https://doi.org/10.1016/S0031-0182(98)00137-0), 1999.
- Bradl, H. B.: Adsorption of heavy metal ions on soils and soils constituents, *J. Colloid Interf. Sci.*, 277, 1–18, <https://doi.org/10.1016/j.jcis.2004.04.005>, 2004.
- Brady, N. C.: The nature and properties of soils, 9th edn., Macmillan/Collier Macmillan, New York, London, 750 pp., ISBN 978-0-02-313340-4, 1984.
- Bronick, C. J. and Lal, R.: Soil structure and management: a review, *Geoderma*, 124, 3–22, <https://doi.org/10.1016/j.geoderma.2004.03.005>, 2005.
- Cabrera-Real, H., Romero-Serrano, A., Zeifert, B., Hernandez-Ramirez, A., Hallen-Lopez, M., and Cruz-Ramirez, A.: Effect of MgO and CaO/SiO<sub>2</sub> on the immobilization of chromium in synthetic slags, *J. Mater. Cycles and Waste*, 14, 317–324, <https://doi.org/10.1007/s10163-012-0072-y>, 2012.
- Calabrese, E. J., Stanek, E. J., James, R. C., and Roberts, S. M.: Soil ingestion: a concern for acute toxicity in children., *Environ. Health Persp.*, 105, 1354–1358, <https://doi.org/10.1289/ehp.971051354>, 1997.
- Campillo-Cora, C., Conde-Cid, M., Arias-Estévez, M., Fernández-Calviño, D., and Alonso-Vega, F.: Specific Adsorption of Heavy Metals in Soils: Individual and Competitive Experiments, *Agronomy*, 10, 1113, <https://doi.org/10.3390/agronomy10081113>, 2020.
- Campos, V.: Trace Elements in Pesticides, *Commun. Soil Sci. Plan.*, 34, 1261–1268, <https://doi.org/10.1081/CSS-120020442>, 2003.
- Casetta, M., Courcot, L., Caillaud, J., Dumoulin, D., Alaimo, V., Cornille, V., Billon, G., Courcot, D., Hermoso, M., and Philippe, S.: Use of potentially toxic elements in sedimentable industrial dust to trace their input in soils (Northern France), *J. Soils Sediments*, 1–21, <https://doi.org/10.1007/s11368-024-03817-7>, 2024.
- Cécillon, L., Baudin, F., Chenu, C., Houot, S., Jolivet, R., Kätterer, T., Lutfalla, S., Macdonald, A., van Oort, F., Plante, A. F., Savignac, F., Soucémarianadin, L. N., and Barré, P.: A model based on Rock-Eval thermal analysis to quantify the size of the centennially persistent organic carbon pool in temperate soils, *Biogeosciences*, 15, 2835–2849, <https://doi.org/10.5194/bg-15-2835-2018>, 2018.
- Chapman, D. V. (Ed.): Water quality assessments: a guide to the use of biota, sediments and water in environmental monitoring, 2nd Edn., E & FN Spon, London, 626 pp., ISBN 978-0-419-21590-5, 1996.
- Chen, C.-W., Kao, C. M., Chen, C.-F., and Dong, C.-D.: Distribution and accumulation of heavy metals in the sediments of Kaohsiung Harbor, Taiwan, *Chemosphere*, 66, 1431–40, <https://doi.org/10.1016/j.chemosphere.2006.09.030>, 2007.
- Chitolina, G. M., Mendes, K. F., Almeida, C. S., Alonso, F. G., Junqueira, L. V., and Tornisiello, V. L.: Influence of Soil Depth on Sorption and Desorption Processes of Hexazinone, *Planta Daninha*, 38, e020217734, <https://doi.org/10.1590/S0100-83582020380100016>, 2020.
- Crea, F., Foti, C., Milea, D., and Sammartano, S.: Speciation of Cadmium in the Environment, in: Cadmium: From Toxicity to Essentiality, edited by: Sigel, A., Sigel, H., and Sigel, R. K., Springer Netherlands, Dordrecht, 63–83, [https://doi.org/10.1007/978-94-007-5179-8\\_3](https://doi.org/10.1007/978-94-007-5179-8_3), 2013.
- Crispo, M., Dobson, M. C., Blevins, R. S., Meredith, W., Lake, J. A., and Edmondson, J. L.: Heavy metals and metalloids concentrations across UK urban horticultural soils and the factors influencing their bioavailability to food crops, *Environ. Pollut.*, 288, 117960, <https://doi.org/10.1016/j.envpol.2021.117960>, 2021.
- DesMarais, T. L. and Costa, M.: Mechanisms of Chromium-Induced Toxicity, *Curr. Opin. Toxicol.*, 14, 1–7, <https://doi.org/10.1016/j.cotox.2019.05.003>, 2019.
- Disnar, J.-R., Guillet, B., Kéravis, D., Di-Giovanni, C., and Sebag, D.: Soil organic matter (SOM) characterization by Rock-Eval pyrolysis, *Org. Geochem.*, 34, 327–343, [https://doi.org/10.1016/S0146-6380\(02\)00239-5](https://doi.org/10.1016/S0146-6380(02)00239-5), 2003.
- Donisa, C., Mocanu, R., and Steinnes, E.: Distribution of some major and minor elements between fulvic and humic acid fractions in natural soils, *Geoderma*, 111, 75–84, [https://doi.org/10.1016/S0016-7061\(02\)00254-9](https://doi.org/10.1016/S0016-7061(02)00254-9), 2003.
- Douay, F., Pelfrène, A., Planque, J., Fourrier, H., Richard, A., Roussel, H., and Girondelot, B.: Assessment of potential health risk for inhabitants living near a former lead smelter. Part 1: metal concentrations in soils, agricultural crops, and home-grown vegetables, *Environ. Monit. Assess.*, 185, 3665–3680, <https://doi.org/10.1007/s10661-012-2818-3>, 2013.
- Dror, I., Yaron, B., and Berkowitz, B.: The Human Impact on All Soil-Forming Factors during the Anthropocene, *ACS Environ. Au*, 2, 11–19, <https://doi.org/10.1021/acsenvironau.1c00010>, 2022.
- Duchaufour, P.: Humification et écologie, *Cahiers ORSTOM, Série Pédologie*, 8, 379–390, 1970.
- Duchaufour, P., Faivre, P., Poulenard, J., and Gury, M.: Introduction à la science du sol: sol, végétation, environnement: licence 3, master, Capes, Dunod, Malakoff (Hauts-de-Seine), ISBN 978-2-10-081992-8, 2020.
- Duodu, G. O., Goonetilleke, A., and Ayoko, G. A.: Potential bioavailability assessment, source apportionment and ecological risk of heavy metals in the sediment of Brisbane River estuary, Australia, *Mar. Pollut. Bull.*, 117, 523–531, <https://doi.org/10.1016/j.marpolbul.2017.02.017>, 2017.
- Duzgoren-Aydin, N. S., Wong, C. S. C., Aydin, A., Song, Z., You, M., and Li, X. D.: Heavy Metal Contamination and Distribution in the Urban Environment of Guangzhou,

- SE China, *Environ. Geochem. Hlth.*, 28, 375–391, <https://doi.org/10.1007/s10653-005-9036-7>, 2006.
- Emadodin, I. and Bork, H. R.: Degradation of soils as a result of long-term human-induced transformation of the environment in Iran: an overview, *J. Land Use Sci.*, 7, 203–219, <https://doi.org/10.1080/1747423X.2011.560292>, 2012.
- Espitalié, J., Laporte, J. L., Madec, M., Marquis, F., Leplat, P., Paulet, J., and Boutefeu, A.: Méthode rapide de caractérisation des roches mères, de leur potentiel pétrolier et de leur degré d'évolution, *Rev. Inst. Fr. Pet. Ann.*, 32, 23–42, <https://doi.org/10.2516/ogst:1977002>, 1977.
- Espitalié, J., Deroo, G., and Marquis, F.: La pyrolyse Rock-Eval et ses applications. Deuxième partie., *Rev. Inst. Fr. Pet. Ann.*, 40, 755–784, <https://doi.org/10.2516/ogst:1985045>, 1985.
- Falson, G., Celi, L., Caimi, A., Simonov, G., and Bonifacio, E.: The effect of clear cutting on podzolisation and soil carbon dynamics in boreal forests (Middle Taiga zone, Russia), *Geoderma*, 177–178, 27–38, <https://doi.org/10.1016/j.geoderma.2012.01.036>, 2012.
- FAO (edn.): World reference base for soil resources 2014: international soil classification system for naming soils and creating legends for soil maps, FAO, Rome, ISBN 978-92-5-108369-7, 2014.
- FAO and UNEP: Global assessment of soil pollution – Summary for policy makers, Rome, FAO, <https://doi.org/10.4060/cb4827en>, 2021.
- Fendorf, S. E.: Surface reactions of chromium in soils and waters, *Geoderma*, 67, 55–71, [https://doi.org/10.1016/0016-7061\(94\)00062-F](https://doi.org/10.1016/0016-7061(94)00062-F), 1995.
- Feng, X., Hong, Y., Hong, B., and Ni, J.: Mobility of some potentially toxic trace elements in the coal of Guizhou, China, *Environ. Geol.*, 39, 372–377, <https://doi.org/10.1007/s002540050016>, 2000.
- Fernández-Turiel, J. L., de Carvalho, W., Cabañas, M., Querol, X., and López-Soler, A.: Mobility of heavy metals from coal fly ash, *Geo*, 23, 264–270, <https://doi.org/10.1007/BF00766741>, 1994.
- Fiedler, S., Vepřaskas, M. J., and Richardson, J. L.: Soil Redox Potential: Importance, Field Measurements, and Observations, in: *Advances in Agronomy*, vol. 94, edited by: Sparks, D. L., Academic Press, 1–54, [https://doi.org/10.1016/S0065-2113\(06\)94001-2](https://doi.org/10.1016/S0065-2113(06)94001-2), 2007.
- Fijałkowski, K., Kacprzak, M., Grobelak, A., and Placek, A.: The influence of selected soil parameters on the mobility of heavy metals in soil, *Inżynieria i Ochrona Środowiska/Engineering and Protection of Environment*, 15, 81–92, 2012.
- Gardner, M., Comber, S., Scrimshaw, M. D., Cartmell, E., Lester, J., and Ellor, B.: The significance of hazardous chemicals in wastewater treatment works effluents, *Sci. Total Environ.*, 437, 363–372, <https://doi.org/10.1016/j.scitotenv.2012.07.086>, 2012.
- Géorisques: Pollution des sols, SIS et anciens sites industriels: <https://www.georisques.gouv.fr/risques/sites-et-sols-pollues/donnees>, last access: 17 April 2023a.
- Géorisques: Registre des émissions polluantes: <https://www.georisques.gouv.fr/risques/registre-des-emissions-polluantes/etablissement/donnees>, last access: 17 April 2023b.
- Girard, M.-C.: Sols et environnement: cours, exercices et études de cas, Dunod, Paris, ISBN 978-2-10-005520-3, 2005.
- GIS Sol and RMT Sols et Territoires: Pédologie – Les sols dominants de France métropolitaine, <https://www.gissol.fr/donnees/carte-sur-le-geoportail-4789> (last access: 9 October 2023), 2019.
- Goix, S., Mombo, S., Schreck, E., Pierart, A., Lévêque, T., Deola, F., and Dumat, C.: Field isotopic study of lead fate and compartmentalization in earthworm–soil–metal particle systems for highly polluted soil near Pb recycling factory, *Chemosphere*, 138, 10–17, <https://doi.org/10.1016/j.chemosphere.2015.05.010>, 2015.
- Goldberg, S., Forster, H. s., and Godfrey, C. I.: Molybdenum Adsorption on Oxides, Clay Minerals, and Soils, *Soil Sci. Soc. Am. J.*, 60, 425–432, <https://doi.org/10.2136/sssaj1996.03615995006000020013x>, 1996.
- Guo, G., Wu, F., Xie, F., and Zhang, R.: Spatial distribution and pollution assessment of heavy metals in urban soils from southwest China, *J. Environ. Sci.*, 24, 410–418, [https://doi.org/10.1016/S1001-0742\(11\)60762-6](https://doi.org/10.1016/S1001-0742(11)60762-6), 2012.
- Hailegnaw, N. S., Bayabil, H. K., Li, Y. C., and Gao, B.: Seawater flooding of calcareous soils: Implications for trace and alkaline metals mobility, *Sci. Total Environ.*, 927, 172210, <https://doi.org/10.1016/j.scitotenv.2024.172210>, 2024.
- Hamdoun, H., Leleyter, L., Van-Veen, E., Coggan, J., Basset, B., Lemoine, M., and Baraud, F.: Comparison of three procedures (single, sequential and kinetic extractions) for mobility assessment of Cu, Pb and Zn in harbour sediments, *CR Geosci.*, 347, 94–102, <https://doi.org/10.1016/j.crte.2015.03.003>, 2015.
- Han, L., Chen, B., Liu, T., and Choi, Y.: Leaching Characteristics of Iron and Manganese from Steel Slag with Repetitive Replenishment of Leachate, *KSCE J. Civ. Eng.*, 23, 3297–3304, <https://doi.org/10.1007/s12205-019-0250-8>, 2019.
- Hanna, K., Lassabatere, L., and Bechet, B.: Zinc and lead transfer in a contaminated roadside soil: Experimental study and modeling, *J. Hazard. Mater.*, 161, 1499–1505, <https://doi.org/10.1016/j.jhazmat.2008.04.124>, 2009.
- Harb, M. K., Ebqa'ai, M., Al-Rashidi, A., Alaziqi, B. H., Al Rashdi, M. S., and Ibrahim, B.: Investigation of selected heavy metals in street and house dust from Al-Qunfudah, Kingdom of Saudi Arabia, *Environ. Earth Sci.*, 74, 1755–1763, 2015.
- He, Z. L., Yang, X. E., and Stoffella, P. J.: Trace elements in agroecosystems and impacts on the environment, *J. Trace Elem. Med. Bio.*, 19, 125–140, <https://doi.org/10.1016/j.jtemb.2005.02.010>, 2005.
- Hernandez-Soriano, M. C. and Jimenez-Lopez, J. C.: Effects of soil water content and organic matter addition on the speciation and bioavailability of heavy metals, *Sci. Total Environ.*, 423, 55–61, <https://doi.org/10.1016/j.scitotenv.2012.02.033>, 2012.
- Hetényi, M. and Nyilas, T.: Soil Organic Matter Characterization Using S3 and S4 Signals from Rock-Eval Pyrolysis, *Pedosphere*, 24, 563–574, [https://doi.org/10.1016/S1002-0160\(14\)60042-4](https://doi.org/10.1016/S1002-0160(14)60042-4), 2014.
- Hleis, D., Fernández-Olmo, I., Ledoux, F., Kfoury, A., Courcot, L., Desmonts, T., and Courcot, D.: Chemical profile identification of fugitive and confined particle emissions from an integrated iron and steelmaking plant, *J. Hazard. Mater.*, 250–251, 246–255, <https://doi.org/10.1016/j.jhazmat.2013.01.080>, 2013.
- Holtzapffel, T.: Les minéraux argileux: préparation, analyse diffractométrique et détermination, Société géologique du Nord, technical publication, 1985.

- Impellitteri, C. A., Lu, Y., Saxe, J. K., Allen, H. E., and Peijnenburg, W. J. G. M.: Correlation of the partitioning of dissolved organic matter fractions with the desorption of Cd, Cu, Ni, Pb and Zn from 18 Dutch soils, *Environ. Int.*, 28, 401–410, [https://doi.org/10.1016/S0160-4120\(02\)00065-X](https://doi.org/10.1016/S0160-4120(02)00065-X), 2002.
- Kandpal, G., Srivastava, P. C., and Ram, B.: Kinetics of Desorption of Heavy Metals from Polluted Soils: Influence of Soil Type and Metal Source, *Water Air Soil Poll.*, 161, 353–363, <https://doi.org/10.1007/s11270-005-5548-0>, 2005.
- Kassambara, A. and Mundt, F.: Extract and Visualize the Results of Multivariate Data Analyses [R package factoextra version 1.0.7], 2020.
- Kfoury, A., Ledoux, F., Roche, C., Delmaire, G., Rousel, G., and Courcot, D.: PM<sub>2.5</sub> source apportionment in a French urban coastal site under steelworks emission influences using constrained non-negative matrix factorization receptor model, *J. Environ. Sci.*, 40, 114–128, <https://doi.org/10.1016/j.jes.2015.10.025>, 2016.
- Khademi, H., Gabarrón, M., Abbaspour, A., Martínez-Martínez, S., Faz, A., and Acosta, J. A.: Environmental impact assessment of industrial activities on heavy metals distribution in street dust and soil, *Chemosphere*, 217, 695–705, <https://doi.org/10.1016/j.chemosphere.2018.11.045>, 2019.
- Kicińska, A.: Physical and chemical characteristics of slag produced during Pb refining and the environmental risk associated with the storage of slag, *Environ. Geochem. Hlth.*, 43, 2723–2741, <https://doi.org/10.1007/s10653-020-00738-5>, 2021.
- King, E. K., Perakis, S. S., and Pett-Ridge, J. C.: Molybdenum isotope fractionation during adsorption to organic matter, *Geochim. Cosmochim. Ac.*, 222, 584–598, <https://doi.org/10.1016/j.gca.2017.11.014>, 2018.
- Kubier, A., Wilkin, R. T., and Pichler, T.: Cadmium in soils and groundwater: A review, *Appl. Geochem.*, 108, 1–16, <https://doi.org/10.1016/j.apgeochem.2019.104388>, 2019.
- Kubová, J., Matúš, P., Bujdoš, M., Hagarová, I., and Medved', J.: Utilization of optimized BCR three-step sequential and dilute HCl single extraction procedures for soil–plant metal transfer predictions in contaminated lands, *Talanta*, 75, 1110–1122, <https://doi.org/10.1016/j.talanta.2008.01.002>, 2008.
- Lafargue, E., Marquis, F., and Pillot, D.: Rock-Eval 6 Applications in Hydrocarbon Exploration, Production, and Soil Contamination Studies, *Rev. Inst. Fr. Pet. Ann.*, 53, 421–437, <https://doi.org/10.2516/ogst:1998036>, 1998.
- Lasota, J., Błońska, E., Łyszczarz, S., and Tibbett, M.: Forest Humus Type Governs Heavy Metal Accumulation in Specific Organic Matter Fractions, *Water Air Soil Poll.*, 231, 80, <https://doi.org/10.1007/s11270-020-4450-0>, 2020.
- Lê, S., Josse, J., and Husson, F.: FactoMineR: A Package for Multivariate Analysis, *J. Stat. Softw.*, 25, 1–18, <https://doi.org/10.18637/jss.v025.i01>, 2008.
- Lee, C. S., Li, X., Shi, W., Cheung, S. C., and Thornton, I.: Metal contamination in urban, suburban, and country park soils of Hong Kong: A study based on GIS and multivariate statistics, *Sci. Total Environ.*, 356, 45–61, <https://doi.org/10.1016/j.scitotenv.2005.03.024>, 2006.
- Leifeld, J. and Kögel-Knabner, I.: Organic carbon and nitrogen in fine soil fractions after treatment with hydrogen peroxide, *Soil Biol. Biochem.*, 33, 2155–2158, [https://doi.org/10.1016/S0038-0717\(01\)00127-4](https://doi.org/10.1016/S0038-0717(01)00127-4), 2001.
- Leplat, J., Sommé, J., Baeteman, C., and Paepe, R.: Carte géologique de la France à 1/50 000 – Dunkerque-Hondschoote, 1988.
- Li, X., Lan, X., Liu, W., Cui, X., and Cui, Z.: Toxicity, migration and transformation characteristics of lead in soil-plant system: Effect of lead species, *J. Hazard. Mater.*, 395, 122676, <https://doi.org/10.1016/j.jhazmat.2020.122676>, 2020.
- Li, Z. and Shuman, L. M.: Heavy metal movement in metal-contaminated soil profiles, *Soil Sci.*, 161, 736–750, <https://doi.org/10.1097/00010694-199610000-00003>, 1996.
- Luo, W. T., Nelson, P. N., Li, M.-H., Cai, J. P., Zhang, Y. Y., Zhang, Y. G., Yang, S., Wang, R. Z., Wang, Z. W., Wu, Y. N., Han, X. G., and Jiang, Y.: Contrasting pH buffering patterns in neutral-alkaline soils along a 3600 km transect in northern China, *Biogeosciences*, 12, 7047–7056, <https://doi.org/10.5194/bg-12-7047-2015>, 2015.
- Madrid, F., Reinoso, R., Florido, M. C., Díaz Barrientos, E., Ajmone-Marsan, F., Davidson, C. M., and Madrid, L.: Estimating the extractability of potentially toxic metals in urban soils: A comparison of several extracting solutions, *Environ. Pollut.*, 147, 713–722, <https://doi.org/10.1016/j.envpol.2006.09.005>, 2007.
- Manta, D. S., Angelone, M., Bellanca, A., Neri, R., and Sprovieri, M.: Heavy metals in urban soils: a case study from the city of Palermo (Sicily), Italy, *Sci. Total Environ.*, 300, 229–243, [https://doi.org/10.1016/S0048-9697\(02\)00273-5](https://doi.org/10.1016/S0048-9697(02)00273-5), 2002.
- Minami, K.: Soil and humanity: Culture, civilization, livelihood and health, *Soil Sci. Plant Nutr.*, 55, 603–615, <https://doi.org/10.1111/j.1747-0765.2009.00401.x>, 2009.
- Mombelli, D., Mapelli, C., Barella, S., Di Cecca, C., Le Saout, G., and Garcia-Diaz, E.: The effect of microstructure on the leaching behaviour of electric arc furnace (EAF) carbon steel slag, *Process Saf. Environ.*, 102, 810–821, <https://doi.org/10.1016/j.psep.2016.05.027>, 2016.
- Ortega Montoya, C. Y., López-Pérez, A. O., Ugalde Monzalvo, M., and Ruvalcaba Sánchez, Ma. L. G.: Multidimensional Urban Exposure Analysis of Industrial Chemical Risk Scenarios in Mexican Metropolitan Areas, *Int. J. Env. Res. Pub. He.*, 18, 5674, <https://doi.org/10.3390/ijerph18115674>, 2021.
- Orucoglu, E., Grangeon, S., Gloter, A., Robinet, J.-C., Madé, B., and Tournassat, C.: Competitive Adsorption Processes at Clay Mineral Surfaces: A Coupled Experimental and Modeling Approach, *ACS Earth Space Chem.*, 6, 144–159, <https://doi.org/10.1021/acsearthspacechem.1c00323>, 2022.
- Otunola, B. O. and Ololade, O. O.: A review on the application of clay minerals as heavy metal adsorbents for remediation purposes, *Environmental Technology and Innovation*, 18, 100692, <https://doi.org/10.1016/j.eti.2020.100692>, 2020.
- Palansooriya, K. N., Shaheen, S. M., Chen, S. S., Tsang, D. C. W., Hashimoto, Y., Hou, D., Bolan, N. S., Rinklebe, J., and Ok, Y. S.: Soil amendments for immobilization of potentially toxic elements in contaminated soils: A critical review, *Environ. Int.*, 134, 105046, <https://doi.org/10.1016/j.envint.2019.105046>, 2020.
- Panagos, P., Ballabio, C., Lugato, E., Jones, A., Borrelli, P., Scarpa, S., Orgiazzi, A., and Montanarella, L.: Potential Sources of Anthropogenic Copper Inputs to European Agricultural Soils, *Sustainability*, 10, 2380, <https://doi.org/10.3390/su10072380>, 2018.
- Pelfrène, A., Sahmer, K., Waterlot, C., Glorennec, P., Douay, F., and Le Bot, B.: Evaluation of single-

- extraction methods to estimate the oral bioaccessibility of metal(loid)s in soils, *Sci. Total Environ.*, 727, 138553, <https://doi.org/10.1016/j.scitotenv.2020.138553>, 2020.
- Pellegrini, E., Contin, M., Mazhar, S., Bravo, C., and De Nobili, M.: Flooding by sea and brackish waters enhances mobility of Cd, Zn and Pb from airborne dusts in coastal soils, *Sci. Total Environ.*, 922, 171038, <https://doi.org/10.1016/j.scitotenv.2024.171038>, 2024.
- Philippe, S., Leterme, C., Lesourd, S., Courcot, L., Haack, U., and Caillaud, J.: Bioavailability of sediment-borne lead for ragworms (*Hediste diversicolor*) investigated by lead isotopes, *Appl. Geochem.*, 23, 2932–2944, <https://doi.org/10.1016/j.apgeochem.2008.04.012>, 2008.
- Preston, C. M. and Schmidt, M. W. I.: Black (pyrogenic) carbon: a synthesis of current knowledge and uncertainties with special consideration of boreal regions, *Biogeosciences*, 3, 397–420, <https://doi.org/10.5194/bg-3-397-2006>, 2006.
- QGIS Development Team: QGIS Geographic Information System, Open Source Geospatial Foundation Project, <https://qgis.org> (last access: 16 March 2023), 2023.
- Querol, X., Fernández-Turiel, J., and López-Soler, A.: Trace elements in coal and their behaviour during combustion in a large power station, *Fuel*, 74, 331–343, [https://doi.org/10.1016/0016-2361\(95\)93464-O](https://doi.org/10.1016/0016-2361(95)93464-O), 1995.
- R Core Team: R: A Language and Environment for Statistical Computing, <https://www.r-project.org> (last access: 16 March 2023), 2022.
- Rajmohan, N., Prathapar, S. A., Jayaprakash, M., and Nagarajan, R.: Vertical distribution of heavy metals in soil profile in a seasonally waterlogging agriculture field in Eastern Ganges Basin, *Environ. Monit. Assess.*, 186, 5411–5427, <https://doi.org/10.1007/s10661-014-3790-x>, 2014.
- Rao, C. R. M., Sahuquillo, A., and Lopez-Sanchez, J. F.: Comparison of single and sequential extraction procedures for the study of rare earth elements remobilisation in different types of soils, *Anal. Chim. Acta*, 662, 128–136, <https://doi.org/10.1016/j.aca.2010.01.006>, 2010.
- Reimann, C. and De Caritat, P.: Chemical elements in the environment: factsheets for the geochemist and environmental scientist, Springer, Berlin, New York, 397 pp., ISBN 978-3-540-63670-0, 1998.
- Ren, Z. L., Sivry, Y., Dai, J., Tharaud, M., Cordier, L., and Benedetti, M. F.: Multi-element stable isotopic dilution and multi-surface modelling to assess the speciation and reactivity of cadmium and copper in soil, *Eur. J. Soil Sci.*, 66, 973–982, <https://doi.org/10.1111/ejss.12298>, 2015.
- Rengasamy, P. and Churchman, G. J.: Cation exchange capacity, exchangeable cations and sodicity, Collingwood, Vic, CSIRO Publishing, ISBN 978-0-643-06376-1, 1999.
- Richer-De-Forges, A. C., Feller, C., Jamagne, M., and Arrouays, D. D.: Perdus dans le triangle des textures, *Etude et Gestion des Sols*, 15, p. 97, 2008.
- Roosa, S., Prygiel, E., Lesven, L., Wattiez, R., Gillan, D., Ferrari, B. J. D., Criquet, J., and Billon, G.: On the bioavailability of trace metals in surface sediments: a combined geochemical and biological approach, *Environ. Sci. Pollut. R.*, 23, 10679–10692, <https://doi.org/10.1007/s11356-016-6198-z>, 2016.
- Saenger, A., Cécillon, L., Sebag, D., and Brun, J.-J.: Soil organic carbon quantity, chemistry and thermal stability in a mountainous landscape: A Rock–Eval pyrolysis survey, *Org. Geochem.*, 54, 101–114, <https://doi.org/10.1016/j.orggeochem.2012.10.008>, 2013.
- dos Santos, J. V., Fregolente, L. G., Mounier, S., Hajjoul, H., Ferreira, O. P., Moreira, A. B., and Bisinoti, M. C.: Fulvic acids from Amazonian anthropogenic soils: Insight into the molecular composition and copper binding properties using fluorescence techniques, *Ecotox. Environ. Safe.*, 205, 111173, <https://doi.org/10.1016/j.ecoenv.2020.111173>, 2020.
- Sarkar, B., Mukhopadhyay, R., Ramanayaka, S., Bolan, N., and Ok, Y. S.: The role of soils in the disposition, sequestration and decontamination of environmental contaminants, *Philos. T. R. Soc. B*, 376, 20200177, <https://doi.org/10.1098/rstb.2020.0177>, 2021.
- Schnitzer, M. and Kerndorff, H.: Reactions of fulvic acid with metal ions, *Water Air Soil Poll.*, 15, 97–108, <https://doi.org/10.1007/BF00285536>, 1981.
- Schulin, R., Curchod, F., Mondeshka, M., Daskalova, A., and Keller, A.: Heavy metal contamination along a soil transect in the vicinity of the iron smelter of Kremikovtzi (Bulgaria), *Geoderma*, 140, 52–61, <https://doi.org/10.1016/j.geoderma.2007.03.007>, 2007.
- Shi, Z., Peltier, E., and Sparks, D. L.: Kinetics of Ni Sorption in Soils: Roles of Soil Organic Matter and Ni Precipitation, *Environ. Sci. Technol.*, 46, 2212–2219, <https://doi.org/10.1021/es202376c>, 2012.
- Smedley, P. L. and Kinniburgh, D. G.: Molybdenum in natural waters: A review of occurrence, distributions and controls, *Appl. Geochem.*, 84, 387–432, <https://doi.org/10.1016/j.apgeochem.2017.05.008>, 2017.
- Smith, P., Cotrufo, M. F., Rumpel, C., Paustian, K., Kuikman, P. J., Elliott, J. A., McDowell, R., Griffiths, R. I., Asakawa, S., Bustamante, M., House, J. I., Sobocká, J., Harper, R., Pan, G., West, P. C., Gerber, J. S., Clark, J. M., Adhya, T., Scholes, R. J., and Scholes, M. C.: Biogeochemical cycles and biodiversity as key drivers of ecosystem services provided by soils, *Soil*, 1, 665–685, <https://doi.org/10.5194/soil-1-665-2015>, 2015.
- Smolders, E. and Degryse, F.: Fate and Effect of Zinc from Tire Debris in Soil, *Environ. Sci. Technol.*, 36, 3706–3710, <https://doi.org/10.1021/es025567p>, 2002.
- Snape, I., Scouller, R. C., Stark, S. C., Stark, J., Riddle, M. J., and Gore, D. B.: Characterisation of the dilute HCl extraction method for the identification of metal contamination in Antarctic marine sediments, *Chemosphere*, 57, 491–504, <https://doi.org/10.1016/j.chemosphere.2004.05.042>, 2004.
- Soil Science Division Staff: Soil survey manual, in: USDA Handbook 18, edited by: Ditzler, C., Scheffe, K., and Monger, H. C., Government Printing Office, Washington, D. C., 639, ISBN 978-016-093743-9, 2017.
- Stavi, I., Bel, G., and Zaady, E.: Soil functions and ecosystem services in conventional, conservation, and integrated agricultural systems. A review, *Agron. Sustain. Dev.*, 36, 32, <https://doi.org/10.1007/s13593-016-0368-8>, 2016.
- Sterckeman, T., Douay, F., Proix, N., and Fourier, H.: Vertical distribution of Cd, Pb and Zn in soils near smelters in the North of France, *Environ. Pollut.*, 107, 377–389, [https://doi.org/10.1016/S0269-7491\(99\)00165-7](https://doi.org/10.1016/S0269-7491(99)00165-7), 2000.
- Sterckeman, T., Douay, F., Baize, D., Fourier, H., Proix, N., and Schwartz, C.: Factors affecting trace element concentrations in

- soils developed on recent marine deposits from northern France, *Appl. Geochem.*, 19, 89–103, [https://doi.org/10.1016/S0883-2927\(03\)00085-4](https://doi.org/10.1016/S0883-2927(03)00085-4), 2004.
- Sun, J., Yu, R., Hu, G., Su, G., and Zhang, Y.: Tracing of heavy metal sources and mobility in a soil depth profile via isotopic variation of Pb and Sr, *Catena*, 171, 440–449, <https://doi.org/10.1016/j.catena.2018.07.040>, 2018.
- Taylor, S. R. and McLennan, S. M.: The geochemical evolution of the continental crust, *Rev. Geophys.*, 33, 241–265, <https://doi.org/10.1029/95RG00262>, 1995.
- Tetteh, R. N.: Chemical soil degradation as a result of contamination: A review, *JSSEM*, 6, 301–308, <https://doi.org/10.5897/JSSEM15.0499>, 2015.
- Townsend, A. T., Palmer, A. S., Stark, S. C., Samson, C., Scouller, R. C., and Snape, I.: Trace metal characterisation of marine sediment reference materials MESS-3 and PACS-2 in dilute HCl extracts, *Mar. Pollut. Bull.*, 54, 236–239, <https://doi.org/10.1016/j.marpolbul.2006.11.002>, 2007.
- Vandenbroucke, M. and Largeau, C.: Kerogen origin, evolution and structure, *Org. Geochem.*, 38, 719–833, <https://doi.org/10.1016/j.orggeochem.2007.01.001>, 2007.
- Varadachari, C., Mondal, A. H., Dulal, C., N., and Ghosh, K.: Clay-humus complexation: Effect of pH and the nature of bonding, *Soil Biol. Biochem.*, 26, 1145–1149, [https://doi.org/10.1016/0038-0717\(94\)90136-8](https://doi.org/10.1016/0038-0717(94)90136-8), 1994.
- Warwick, P., Hall, A., Pashley, V., Van der Lee, J., and Maes, A.: Zinc and cadmium mobility in sand: effects of pH, speciation, Cation Exchange Capacity (CEC), humic acid and metal ions, *Chemosphere*, 36, 2283–2290, [https://doi.org/10.1016/S0045-6535\(97\)10197-7](https://doi.org/10.1016/S0045-6535(97)10197-7), 1998.
- Waterlot, C., Douay, F., and Pelfrène, A.: Chemical Availability of Cd, Pb and Zn in Anthropogenically Polluted Soil: Assessing the Geochemical Reactivity and Oral Bioaccessibility, *Pedosphere*, 27, 616–629, [https://doi.org/10.1016/S1002-0160\(17\)60356-4](https://doi.org/10.1016/S1002-0160(17)60356-4), 2017.
- Wei, T. and Simko, V.: R package “corrplot”: Visualization of a Correlation Matrix, <https://CRAN.R-project.org/package=corrplot> (last access: 16 March 2023), 2021.
- Wickham, H.: *ggplot2: Elegant Graphics for Data Analysis*, 2nd edn. 2016, Springer International Publishing: Imprint: Springer, Cham, 1 pp., <https://doi.org/10.1007/978-3-319-24277-4>, 2016.
- Williams, D. E., Vlamis, J., Pukite, A. H., and Corey, J. E.: Metal movement in sludge-amended soils: A nine-year study, *Soil Sci.*, 143, 124–131, <https://doi.org/10.1097/00010694-198702000-00007>, 1987.
- Ye, C., Li, S., Zhang, Y., and Zhang, Q.: Assessing soil heavy metal pollution in the water-level-fluctuation zone of the Three Gorges Reservoir, China, *J. Hazard. Mater.*, 191, 366–372, <https://doi.org/10.1016/j.jhazmat.2011.04.090>, 2011.
- Yong, R. N., Mohamed, A.-M. O., and Warkentin, B. P.: *Principles of contaminant transport in soils*, Elsevier, Amsterdam; New York, 327 pp., ISBN 978-0-444-88293-6, 1992.
- Yu, D., Qiu, W., Zhang, Z., Glass, K., Su, J., DeMeo, D. L., Tantisira, K., and Weiss, S. T.: corTest: Robust Tests for Equal Correlation, <https://CRAN.R-project.org/package=corTes> (last access: 16 March 2023), 2020.
- Yu, H., Li, C., Yan, J., Ma, Y., Zhou, X., Yu, W., Kan, H., Meng, Q., Xie, R., and Dong, P.: A review on adsorption characteristics and influencing mechanism of heavy metals in farmland soil, *RSC Adv.*, 13, 3505–3519, <https://doi.org/10.1039/D2RA07095B>, 2023.
- Yu, Z., Liu, E., Lin, Q., Zhang, E., Yang, F., Wei, C., and Shen, J.: Comprehensive assessment of heavy metal pollution and ecological risk in lake sediment by combining total concentration and chemical partitioning, *Environ. Pollut.*, 269, 116212, <https://doi.org/10.1016/j.envpol.2020.116212>, 2021.
- Zhao, S., Duan, Y., Lu, J., Gupta, R., Pudasainee, D., Liu, S., Liu, M., and Lu, J.: Chemical speciation and leaching characteristics of hazardous trace elements in coal and fly ash from coal-fired power plants, *Fuel*, 232, 463–469, <https://doi.org/10.1016/j.fuel.2018.05.135>, 2018.
- Zhuang, P., McBride, M. B., Xia, H., Li, N., and Li, Z.: Health risk from heavy metals via consumption of food crops in the vicinity of Dabaoshan mine, South China, *Sci. Total Environ.*, 407, 1551–1561, <https://doi.org/10.1016/j.scitotenv.2008.10.061>, 2009.